UNIVERSIDADE DA CORUÑA
FACULTADE DE CIENCIAS

Bachelor in Chemistry

Final Degree Dissertation Memory

Acidity constants and red-ox potentials calculation of carborane derivatives using electronic structure calculations

Constantes de acidez e potenciais red-ox de compostos derivados dos carboranos mediante cálculos de estrutura electrónica

Constantes de acidez y potenciales red-ox de compuestos derivados de los carboranos mediante cálculos de estructura electrónica

Directors: Juan Arturo Santaballa López
Moisés Canle López

PABLO GROBAS ILLOBRE

Course: 2017/2018 – Convocatory: June

INDEX

ABSTRACT

Carboranes, clusters composed of boron, carbon and hydrogens, show unique physical and chemical properties having application on cancer treatments. Computational Chemistry, a tool to assist in solving chemical problems, has been used to calculate structure, acidity constants and one-electron reduction potentials of carboxyl functionalized carboranes.

Those physico-chemical properties as well as geometry, electronic parameters and IR spectra have been calculated for 1,2-closo-dicarbadodecaborane-1,2-dicarboxylic acid, 1,7-closo-dicarbadodecaborane-1,7-dicarboxylic acid, 1,12-closo-dicarbadodecaborane-1,12-dicarboxylic acid, benzoic acid, phthalic, isophthalic and terephthalic acids and that of their corresponding anions after the first and the second deprotonation - the latter four acids for comparison purposes. Density functional theory (DFT) was used with 6-31++G(d,p) as basis set, and the solvation model based on density (SMD) to simulate the solvent, water.

Structure and characteristics of the most stable species, in terms of Gibbs free energy, were obtained after the corresponding conformational study (PES), which showed that, except for *ortho*-derivatives, all conformers have similar energy. Selected geometric parameters (distances and angles) and electronic parameters (dipole moments and Mulliken atomic charges) including frontier molecular orbitals, are reported. Similar behaviour is observed when comparing phthalic acids and carborane dicarboxylic acids.

Acidity constants were calculated using six different methods, some of them involving a thermodynamic cycle with calculation in the gas phase and in water. No real improvement was found using a more complete basis set. Best results were obtained using a thermodynamic cycle with calculation in the gas phase and in water taking into account empirical values for the solvation energy of water and hydronium ion. Carborane dicarboxylic acids are more acidic, *ca.* 4 pK units, than phthalic acids. On the other hand, one-electron reduction potentials were calculated using two methods, one involving a thermodynamic cycle also. Selected values are reported. Loss of CO_2 by the dianion of *p*-carborane dicarboxylic acid upon one-electron oxidation should be highlighted.

Keywords: *carborane, carborane dicarboxylic acids, phthalic acids, benzoic acid, Computational Chemistry, Quantum Mechanics, Density Functional Theory (DFT), basis set, solvation model based on density (SMD), model chemistry, potential energy surface (PES), geometry optimization, acidity constants, pK_a, one-electron reduction potential.*

RESUMO

Os carboranos, clústeres compostos de boro, carbono e hidróxenos, amosan propiedades físicas e químicas únicas que teñen aplicación en tratamentos contra o cancro. A Química Computacional, unha ferramenta de gran axuda para resolver problemas químicos, utilizouse para calcular a estrutura, as constantes de acidez e os potenciais de redución monoelectrónicos de carboranos funcionalizados con carboxilo.

Calculáronse as propiedades fisicoquímicas, así como a xeometría, os parámetros electrónicos e os espectros IR para o ácido 1,2-closo-dicarbadodecaborano-1,2-dicarboxílico, ácido 1,7-closo-dicarbadodecaborano-1,7-dicarboxílico, ácido 1,12-closo-dicarbadodecaborano-1,12-dicarboxílico, ácido benzoico, ácido ftálico, ácido isoftálico e ácido tereftálico e os dos seus correspondentes anións despois da primeira e segunda desprotonación, estes últimos catro ácidos para propósitos de comparación.

A teoría funcional de densidade (DFT) usouse co 6-31++G(d,p) como función base, e o modelo de solvatación baseado na densidade (SMD) para simular o disolvente, auga.

A estrutura e as características das especies máis estables, en termos de enerxía libre de Gibbs, obtivéronse despois do correspondente estudo conformacional (PES), que amosou que, a excepción dos *orto*-derivados, todos os confórmeros teñen una enerxía similar. Infórmase sobre parámetros xeométricos seleccionados (distancias e ángulos) e parámetros electrónicos (momentos dipolares e cargas atómicas de Mulliken), incluídos os orbitais moleculares de fronteira. Obsérvase un comportamento similar cando se comparan os ácidos ftálicos e os ácidos dicarboxílicos de carborano.

As constantes de acidez calculáronse utilizando seis métodos diferentes, algún dos cales implican un ciclo termodinámico con cálculo na fase gaseosa e en auga. Non se atopou una mellora real empregando unha función base máis completa. Os mellores resultados obtivéronse usando un ciclo termodinámico con cálculo na fase gaseosa e en auga, tendo en conta os valores empíricos para a enerxía de solvatación da auga e o ión hidronio. Os ácidos dicarboxílicos de carboranos son máis ácidos, *aprox.* 4 unidades de pK, que os ácidos ftálicos. Por outro lado, os potenciais de redución monoelectrónicos calculáronse utilizando dous métodos, un que tamén involucra un ciclo termodinámico. Os valores seleccionados infórmanse. Debe resaltarse a perda de CO_2 polo dianión do ácido *p*-carborano dicarboxílico tras a oxidación dun electrón.

Palabras chave: *carboranos, ácidos carborano dicarboxílicos, ácidos ftálicos, ácido benzoico, Química Computacional, Mecánica Cuántica, Teoría do Funcional da Densidade (DFT), funcións base, modelo de solvatación baseado na densidade (SMD), modelo químico, superficie de enerxía potencial (PES), optimización xeométrica, constantes de acidez, pK_a, potenciais de redución monoelectrónicos.*

RESUMEN

Los carboranos, clústeres compuestos de boro, carbono e hidrógenos, muestran propiedades físicas y químicas únicas que tienen aplicación en tratamientos contra el cáncer. La Química Computacional, una herramienta de gran ayuda para resolver problemas químicos, se ha utilizado para calcular la estructura, las constantes de acidez y los potenciales de reducción monoelectrónicos de carboranos funcionalizados con grupos carboxilo.

Se han calculado las propiedades fisicoquímicas, así como la geometría, los parámetros electrónicos y los espectros IR para el ácido 1,2-closo-dicarbadodecaborano-1,2-dicarboxílico, ácido 1,7-closo-dicarbadodecaborano-1,7-dicarboxílico, ácido 1,12-closo-dicarbadodecaborano-1,12-dicarboxílico, ácido benzoico, ácido ftálico, ácido isoftálico y ácido tereftálico y los de sus correspondientes aniones después de la primera y la segunda desprotonación, estos últimos cuatro ácidos para propósitos de comparación. La teoría funcional de densidad (DFT) se usó con 6-31++G(d,p) como función base, y el modelo de solvatación basado en la densidad (SMD) para simular el disolvente, agua. La estructura y las características de las especies más estables, en términos de energía libre de Gibbs, se obtuvieron después del correspondiente estudio conformacional (PES), que mostró que, a excepción de los *orto*-derivados, todos los confórmeros tienen una energía similar. Se informa sobre parámetros geométricos seleccionados (distancias y ángulos) y parámetros electrónicos (momentos dipolares y cargas atómicas de Mulliken), incluidos los orbitales moleculares de frontera. Se observa un comportamiento similar cuando se comparan los ácidos ftálicos y los ácidos dicarboxílicos de carborano.

Las constantes de acidez se calcularon utilizando seis métodos diferentes, algunos de los cuales implican un ciclo termodinámico con cálculo en la fase gaseosa y en agua. No se encontró una mejora real usando una función base más completa. Los mejores resultados se obtuvieron utilizando un ciclo termodinámico con cálculo en la fase gaseosa y en agua, teniendo en cuenta los valores empíricos para la energía de solvatación del agua y el ion hidronio. Los ácidos dicarboxílicos de carboranos son más ácidos, *aprox.* 4 unidades de pK, que los ácidos ftálicos. Por otro lado, los potenciales de reducción monoelectrónicos se calcularon utilizando dos métodos, uno que también involucra un ciclo termodinámico. Los valores seleccionados se informan. Debe resaltarse la pérdida de CO_2 por el dianión del ácido p-carborano dicarboxílico tras la oxidación de un electrón.

Palabras clave: *carboranos, ácidos carborano dicarboxílicos, ácidos ftálicos, ácido benzoico, Química Computacional, Mecánica Cuántica, Teoría del Funcional de la Densidad (DFT), funciones base, modelo de solvatación basado en la densidad (SMD), modelo químico, superficie de energía potencial (PES), optimización geométrica, constantes de acidez, pK_a, potenciales de reducción monoelectrónicos.*

1. INTRODUCTION

Although carboranes have been known for more than a half century, it was not until recently when the interest about them has grown significantly due to their unique physical and chemical properties. Traditionally their use has been centered on cancer treatments, giving promising results.[iii] They are clusters composed of boron, carbon and hydrogen atoms.

Available computing facilities allow the study of chemical compounds in the framework of Quantum Mechanics, thus providing a tool (Computational Chemistry) to assist in solving chemical problems. Current programs allow the calculation, among others, of molecular structures, molecular orbitals, electronic parameters like atomic charges and dipole moments as well as IR spectra, acidity constants and one-electron reduction potentials, and, although out of scope of this work, reaction rate constants. One of the features of Computational Chemistry is the ability to simulate conditions difficult to achieve in the laboratory and analyze species not easy to synthesize.

The functionalized dicarbadodecarboranes, hereafter carborane dicarboxylic acids, have been be studied:

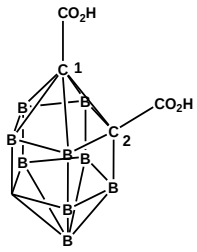

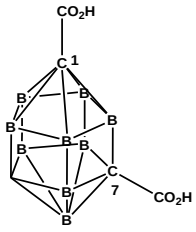

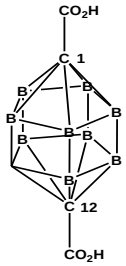

where all H atoms bonded to boron has been suppressed for sake of clarity.

In addition to geometric, electronic parameters and IR spectra, both acidity constants of these compounds have been calculated, using six methods, and compared to that of phthalic acids using electronic structure calculations with the Density of Functional Theory (DFT). Water as a solvent was simulated using the solvation model based on density (SMD). Moreover, one-electron reduction potentials for selected carborane dicarboxylic acids and its monoanion and dianion have been estimated.

This work is organized in nine chapters. The objectives of the work are described after this introduction. Chapter 3 contains a brief introduction on carboranes and the basics of Quantum Chemistry; then materials and methods are described. The work plan appears in chapter 5, and after it the chapter containing the obtained results and the corresponding discussion. Conclusions are collected in chapter 7. References and annexes close this work.

2. OBJECTIVES

The main objective of this work is the calculation of acidity constants and one-electron reduction potentials of *ortho*-, *meta*- and *para*-isomers of carborane dicarboxylic acids. Their achievement implies the following minor objectives:

- Familiarization with the use of bibliographic managers.
- Critical reading of selected literature.
- Learn to manage the Finis Terrae II supercomputer (CESGA).
- Use of computer modeling programs (Gaussian16, Gaussian09, GaussView, GabeEdit, Mercury).
- Learn the fundamentals of Computational Chemistry.
- Optimization of geometry and energy of carborane dicarboxylic acids, phthalic acids and benzoic acid.
- Determination of acidity constants and one-electron reduction potentials.
- Critical analysis of the results.
- Integration between calculations with the different concepts and theories of relevance in chemistry.

3. ANTECEDENTS

3.1 Carboranes

3.1.1 Introduction and history

Carboranes (named “carbaboranes” in formal nomenclature) are polyhedral boron-carbon molecular clusters stabilized by electron-delocalized covalent bonding in the skeletal framework. In contrast to classical organoboranes such as borabenzene (C_5H_5B), the skeletal carbon atoms in carboranes typically have at least three and as many as five or six neighbors in the cluster, forming stable -in some cases, extremely stable- molecular structures. Carboranes have been known for more than a half century but for much of that time they were of interest primarily to boron chemists, theoreticians interested in their structures and bonding, and small groups of industrial researchers, who recognized their potential for creating extremely heat-stable polymers[i,ii]

Carborane chemistry is experiencing a major surge in interest across a wide spectrum of technologies.[i] Because of their unique physical and chemical properties, carboranes have been used to prepare catalysts, radiopharmaceuticals polymers, and an assortment of unique coordination compounds. The medicinal chemistry of carboranes has traditionally centered on their use in boron neutron capture therapy (BNCT), which is a binary therapy modality for treating cancer.[iii] One important class of boron compounds are the polyhedral borane clusters, and these are also being exploited in drug design, particularly in view of their relationship to the more traditional carbopolycyclic scaffolds.[iv]

3.2 Structure and Bonding

3.2.1 Structural patterns in boron clusters

Carboranes are clusters composed of boron, carbon and hydrogen atoms. The range of composition in carborane cages extends from boron-rich clusters to systems having as many as six skeletal carbon atoms, but those with high boron content are dominant. Consequently, in most theoretical treatments of structure and bonding, carboranes are treated as polyhedral boranes in which one or more skeletal boron atoms are replaced by carbon.

Like many related boranes, they are polyhedral and are similarly classified as *closo-, nido-, arachno-, hypho-,* etc. based on whether they represent a complete polyhedron (*closo*-), or a polyhedron that is missing one (*nido*-), two (*arachno*), or more vertices. The

number of valence electrons in carbon atom is equal to those of boron atom plus a hydrogen atom; hence, BH unit can be substituted by carbon in carboranes.

Carboranes are classified as follows:

1. *Closo*-structures are adopted by borane anions $B_nH_n^{-2}$ (n=6 $\rightarrow$12), carboranes $C_2B_{n-2}H_n$ (n=5$\rightarrow$12), and related isoelectronic species. Their n skeletal boron (or carbon) atoms define the vertices of the triangular-faced polyhedra.

   The same polyhedral serve as the basis for the structures of *nido* and *arachno* compounds, too, although for these boranes and carboranes the polyhedra are incomplete.
2. *Nido* structures are adopted by neutral boranes B_nH_{n+4}, carboranes $CB_{n-1}H_{n+3}$, $C_2B_{n-2}H_{n+2}$, $C_3B_{n-3}H_{n+1}$ and $C_4B_{n-4}H_n$ and related ionic species, whose n skeletal boron (or carbon) atoms occupy all but one of the vertices of the appropriate (n+1)-vertex polyhedron.
3. *Arachno* structures are adopted by boranes B_nH_{n+6} and isoelectronic carboranes $C_2B_{n-2}H_{n+4}$ etc. Their n skeletal atoms define all but 2 of the vertices of the appropriate (n+2) vertex polyhedron.
4. *Hypho*- Carboranes ($C_2B_{n-2}H_{n+6}$): three vertices are missing from parent *closo* carborane.
5. *Conjuncto*-Carboranes (from Latin: join together): conjuncto carboranes are formed by joining two or more preceding types.[ii]

Wade's rules are used to rationalize the shape of borane clusters by calculating the total number of skeletal electron pairs (SEP) available for cluster bonding and to understand structural relationship of various boranes.[v]

In all types of carboranes, different isomers are possible by varying the location of the skeletal carbon atoms, and in many cases, isomerism has been observed. Beyond the size, shape, and carbon locations, other variations are possible. The introduction of functional groups at carbon and boron vertexes adds yet another dimension, linking carborane and organic chemistry.

There is an intrinsic property of carboranes whose significance and potential are so far-reaching that it impacts virtually every field of chemistry. This is their extraordinary ability (shared with polyhedral boranes in general) to accommodate metal and nonmetal atoms of nearly every description in the cage framework. Excepting only the extremely electronegative and electropositive elements and the Group 18 gases, carboranes incorporating almost every element in the Periodic Table have been prepared and characterized.[i]

The basic principles of bonding in boron clusters are well understood after decades of study, and in recent years, the advent of density functional theory (DFT) and other powerful computational tools has led to major advances in the correlation of electronic structures with geometry, reactivity, bond strength, NMR shifts and coupling constants, vibrational frequencies, and other properties.[i,ii]

3.3 Computational Chemistry

3.3.1 Introduction

Computational quantum chemistry is a branch of theoretical chemistry whose major goal is to create efficient mathematical approximations and computer programs to calculate the properties of molecules such as their total energy, dipole moments and/or reactivity among others.[vi] Computational chemistry has become a useful way to investigate materials that are too difficult to find or too expensive to purchase. It also helps chemists make predictions before running the actual experiments, so that they can be better prepared for making observations, being a less costly and safer alternative.[vii]

Theoretical chemistry may be defined as a mathematical description of chemistry, whereas computational chemistry is usually used when a mathematical method is sufficiently well developed that it can be properties of molecules a computer.[vi]

Very few aspects of chemistry can be computed exactly, but almost every aspect of chemistry has been described in a qualitative or approximate quantitative computational scheme. While the ability to use modern quantum chemistry software packages is no longer dependent on a detailed understanding of quantum mechanics, there is, nevertheless, a considerable benefit to be gained from a basic knowledge of quantum chemistry and some familiarity with the procedures used in the computer programs. [vii]

There are a number of software packages available for electronic structure calculations and molecular visualization, the majority of which are relatively user-friendly. An example is that used in this work, Gaussian 16 package, which is usually associated to its parent visualization program GaussView.

3.3.2 Model chemistries

A model chemistry is a numerical technique used to explore chemistry on a computer. It can be generalized into three broad categories: *ab initio* (Latin for "from scratch"), semi-empirical and molecular mechanics, as summarized in **Table 1**.

Important characteristics of the models used in computational chemistry are:

a) Level of simplification: very simple to very complex
b) Generality: general or specific, i.e. relate only to specific systems or problems
c) Limitations: one must always be aware of the range of applicability and limits of accuracy of any model.
d) Cost and efficiency: CPU time, memory, disk space[viii]

Fig. 1 shows a visual comparation of different modelling methods for molecules taking into account the accuracy of the calculation vs the number of atoms to which the model is applicable:

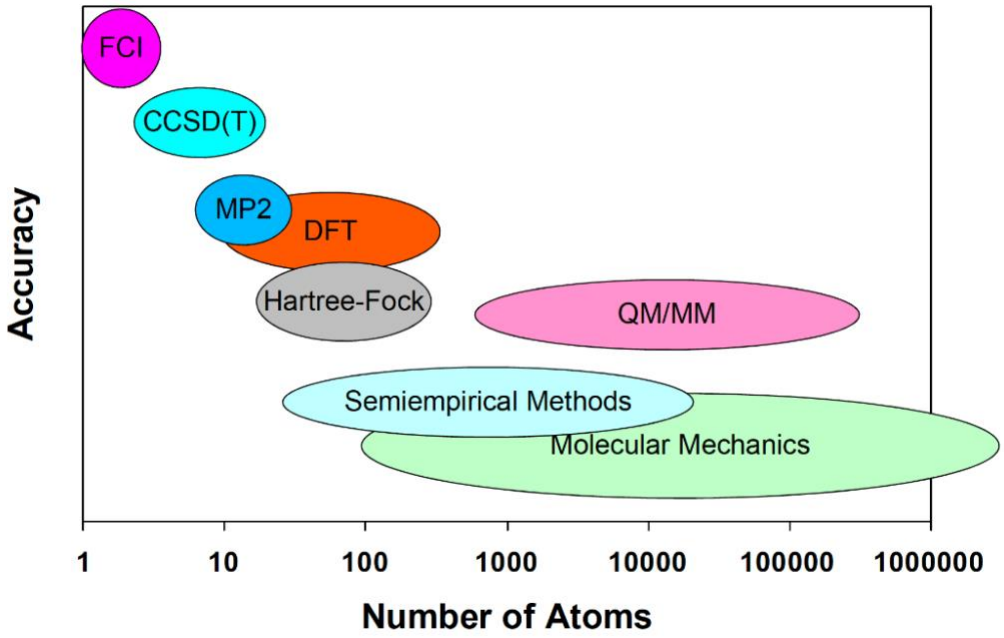

Figure 1. Accuracy of modelling methods and their relation with the number of atoms to which they are applied.[ix]

Table 1. Summary and important aspects of the various techniques used in computational chemistry. [vii]

Technique	Features	Advantages	Disadvantages	Best for
Molecular Mechanics	• Uses classical physics • Relies on force-field with embedded empirical parameters • Computationally least intensive fast and useful with limited computer resources • Can be used for molecules as large as enzymes	• Relies on potentials that have to be somehow supplied • Sometimes inaccurate because the supplied potentials are used beyond their proven range of validity	• Particular force field, applicable only for a limited class of molecules • Does not calculate electronic properties • Requires experimental data (or data from ab initio calculations)	• Large systems • (~1000 of atoms) • Systems or processes with no breaking or forming of bonds
Semi-Empirical	• Uses quantum physics • Uses experimentally derived empirical parameters • Uses many approximation	• Less demanding computationally than ab initio methods • Capable of calculating transition states and excited states	• Requires experimental data (or data from ab initio) for parameters • Less rigorous than ab initio) methods	• Medium-sized systems (hundreds of atoms) • Systems involving electronic transition
Ab initio	• Uses quantum physics • Mathematically rigorous, no empirical parameters • Uses approximation extensively	• Useful for a broad range of systems does not depend on experimental data • Capable of calculating transition states and excited states	• Computationally expensive	• Small systems (tens of atoms) • Systems involving electronic transition • Molecules without available experimental data • Systems requiring rigorous accuracy

3.3.3 Summary of theoretical quantum mechanics

Quantum chemistry requires the solution of the time-independent Schrödinger equation:

$$\hat{H}\psi(R_1, R_2 \ldots R_N, r_1, r_2 \ldots r_n) = E\psi(R_1, R_2 \ldots R_N, r_1, r_2 \ldots r_n), \qquad (1.1)$$

where $\hat{H}$ is the Hamiltonian operator, $\psi(R_1, R_2 \ldots R_N, r_1, r_2 \ldots r_n)$ is the wavefunction for all of the nuclei and electrons, and E is the energy associated with this wavefunction. The Hamiltonian contains all operators that describe the kinetic and potential energy of the molecule at hand. The wavefunction is a function of the nuclear positions R and the electron positions r. Schrödinger equation cannot be exactly solved for molecular systems, so a number of approximations are required to solve it.[x]

3.4 Approximations to the Schrödinger Equation: the Hartree-Fock Method

3.4.1 Nonrelativistic mechanics

Dirac achieved the combination of quantum mechanics and relativity. However, for typical organic molecules, which contain only first- and second-row elements, a relativistic treatment is unnecessary. The complete nonrelativistic Hamiltonian for a molecule consisting of n electrons and N nuclei is given by:

$$\hat{H} = -\frac{h^2}{2}\sum_{I}^{N}\frac{\nabla_I^2}{m_I} - \frac{h^2}{2m_e}\sum_{i}^{n}\nabla_I^2 - \sum_{i}^{n}\sum_{I}^{N}\frac{Z_I e'^2}{r_{Ii}} + \sum_{I>J}^{N}\frac{Z_I Z_J e'^2}{r_{IJ}} + \sum_{i<j}^{n}\frac{e'^2}{r_{ij}}, \qquad (1.2)$$

where

$$e'^2 = \frac{e^2}{4\pi\mathcal{E}_0}. \qquad (1.3)$$

and the lower-case indexes the electrons and the upper-case indexes the nuclei, h is Planck's constant, m_e is the electron mass, m_I is the mass of nucleus I, and r is a distance between the objects specified by the subscript.[x]

3.4.2 Born Oppenheimer approximation

The total molecular wavefunction $\psi(R, r)$ depends on both the positions of all of the nuclei and the positions of all of the electrons. Because electrons are much lighter than nuclei, and therefore move much more rapidly, electrons can essentially instantaneously

respond to any changes in the relative positions of the nuclei. This allows for the separation of the nuclear and electron variables:

$$\psi(R_1, R_2 \dots R_N, r_1, r_2 \dots r_n) = \phi(R_1, R_2 \dots R_N)\psi(r_1, r_2 \dots r_n). \qquad (1.4)$$

This approximation was proposed by Born and Oppenheimer and is valid for the vast majority of organic molecules. The non-relativistic Hamiltonian obtained after applying the Born–Oppenheimer is:

$$\hat{H} = -\frac{1}{2}\sum_{i}^{n} \nabla_I^2 - \sum_{i}^{n}\sum_{I}^{N} \frac{Z_I}{r_{Ii}} + \sum_{i<j}^{n} \frac{1}{r_{ij}} + V^{nuc} \qquad (1.5)$$

where V^{nuc} is the nuclear–nuclear repulsion energy. Equation (1.5) is expressed in atomic units (special system of units used in quantum chemical calculations). The next task is to solve the Schrödinger equation (1.1) with the Hamiltonian expressed in Eq. (1.5).

The potential energy surface (PES) is a central concept in computational chemistry. It is created by the calculation of the electronic energy of a molecule while varying the positions of its nuclei (**Fig. 2**). It is important to recognize that the concept of the PES relies upon the validity of the Born–Oppenheimer approximation.[x]

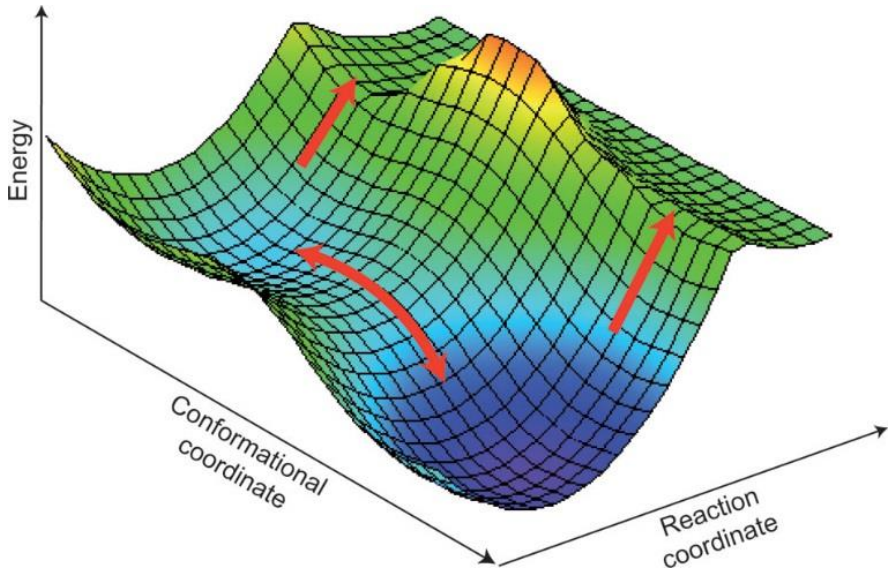

Figure 2. Example of PES graphic with the electronic energy as function of the reaction coordinate.[xi]

3.4.3 *The one-electron wavefunction and the Hartree–Fock method*

The wavefunction ψ(r) depends on the coordinates of all of the electrons in the molecule. Hartree proposed the idea, based on the Born-Oppenheimer approximation, that the electronic wavefunction can be separated into a product of functions that depend only on one electron,

$$\psi(r_1, r_2 \ldots r_n) = \varphi_1(r_1)\varphi_2(r_2) \ldots \varphi_n(r_n). \qquad (1.6)$$

This wavefunction would solve the Schrödinger equation exactly if it were not for the electron–electron repulsion term of the Hamiltonian in Eq. (1.5). Hartree replaced the exact electron– electron repulsion with an effective field V_i^{eff} produced by the average positions of the remaining electrons, with this assumption, the separable functions ϕ_i satisfy the Hartree equations, one for each electron:

$$\left(-\frac{1}{2}\nabla_i^2 - \sum_I^N \frac{Z_I}{r_{Ii}} + V_i^{eff}\right)\varphi_i = E_i\varphi_i. \qquad (1.7)$$

Solving for the set of functions ϕ_i is nontrivial because V_i^{eff} itself depends on all of the functions ϕ_i. An iterative scheme is needed to solve the Hartree equations. First, a set of functions (ϕ_1, ϕ_2 ... ϕ_n) is assumed. These are used to produce the set of effective potential operators V_i^{eff} and the Hartree equations are solved to produce a set of improved functions ϕ_i. These new functions produce an updated effective potential, which in turn yields a new set of functions ϕ. This process is continued until the functions ϕ_i no longer change, resulting in a self-consistent field (SCF).

Hatree's procedure neglects entirely the ability of the electrons to rapidly (essentially instantaneously) respond to the position of other electrons. Fock recognized that the separable wavefunction employed by Hartree (Eq. 1.6) does not satisfy the Pauli Exclusion Principle. Instead, Fock suggested using the Slater determinant

$$\psi(r_1, r_2 \ldots r_n) = \frac{1}{\sqrt{n!}}\begin{vmatrix} \varphi_1(e_1) & \varphi_2(e_1) & \ldots & \varphi_n(e_1) \\ \varphi_1(e_2) & \varphi_2(e_2) & \ldots & \varphi_n(e_2) \\ \vdots & \vdots & & \vdots \\ \varphi_1(e_n) & \varphi_2(e_n) & & \varphi_n(e_n) \end{vmatrix} = |\varphi_1, \varphi_2 \ldots \quad \varphi_n|, \qquad (1.8)$$

which is antisymmetric and satisfies the Pauli Principle. Again, an effective potential is employed, and an iterative scheme provides the solution to the Hartree–Fock (HF) equation;[x] although a detailed explanation of this procedure is beyond the scope of this work, **Fig. 3** shows its main steps.

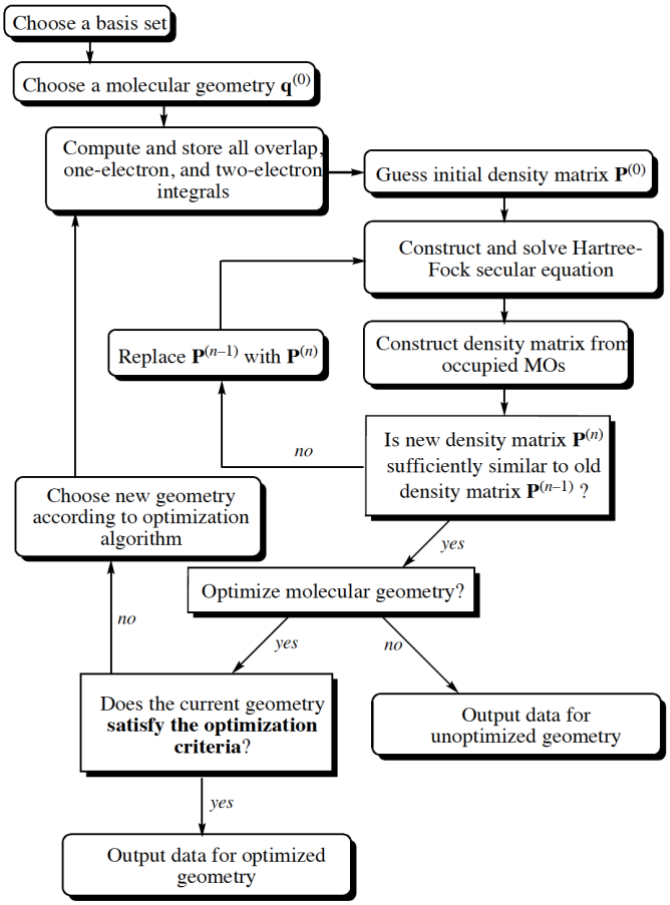

Figure 3. Flowchart for the steps involved in the Hartree-Fock procedure[xii]

Hartree-Fock method is an example of *ab initio* methods. Other methods have been developed to improve the results obtained from HF by accounting for the correlation energy. These are called Post-Hartree-Fock. **Table 2** lists the most popular classes of *ab initio* electronic structure methods.

Table 2. Most popular classes of *ab initio* electronic structure methods[xiii]

Hartree-Fock methods	- Restricted Hartree-Fock (RHF): singlets - Unrestricted Hartree-Fock (UHF): higher multiplicities - Restricted open-shell Hartree-Fock (ROHF)
Post Hartree-Fock methods	- Møller-Plesset perturbation theory (MPn) - Configuration interaction (CI) - Coupled cluster (CC)
Multi-reference methods	- Multi-configurational self-consistent field (MCSCF) - Multi-reference configuration interaction (MRCI) - n-electron valence state perturbation theory (NEVPT) - Complete active space perturbation theory (CASPTn)

3.4.4 *Linear Combination of Atomic Orbitals (LCAO) approximation*

The solutions to the Hartree–Fock model, ϕ_i, are known as the molecular orbitals (MOs). These orbitals generally span the entire molecule, just as the atomic orbitals (AOs) span the space about an atom. Usually chemists consider the atomic properties of atoms to still persist to some extent when embedded within a molecule, it seems reasonable to construct the MOs as an expansion of the AOs,

$$\varphi_i = \sum_{\mu}^{k} C_{i\mu}\chi_{\mu}, \qquad (1.9)$$

where the index μ spans all of the atomic orbitals χ of every atom in the molecule (a total of k atomic orbitals), and $c_{i\mu}$ is the expansion coefficient of AO χμ in MO ϕ_i. Equation (1.9) thus defines the linear combination of atomic orbitals (LCAO) approximation.[x]

3.4.5 *Restricted vs. unrestricted wavefunctions*

The wavefunction for an individual electron describes its spatial extent along with its spin. The electron can be either spin up (α) or spin down (β). For the closed-shell wavefunction, each pair of electrons shares the same spatial orbital but each has a unique spin—one up and the other down (**Fig. 4**). This type of wavefunction is also called a (spin) restricted wavefunction, leading to the restricted Hartree–Fock (RHF) method. When applied to open-shell systems, this is called restricted open-shell HF (ROHF).
This restriction is not demanded. It is a simple way to satisfy the exclusion principle, but it is not the only means for doing so. In an unrestricted wavefunction (UHF) the spin-up electron and its spin-down partner do not have the same spatial description. The Hartree–Fock–Roothaan procedure is slightly modified to handle this case by creating a set of equations for the α electrons and another set for the β electrons.[x]

RHF The spatial parts of the spin orbitals are the **same**	**UHF** The spatial parts of the spin orbitals are **different**

Figure 4. Situation of the α and β electrons when working with the RHF and UHF methods[xiv]

3.5 Basis Sets

To solve for the energy and wavefunction within the Hartree–Fock– Roothaan procedure, the atomic orbitals must be specified. If the set of atomic orbitals is infinite, then the variational principle tells us that we will obtain the lowest possible energy within the HF-SCF method. This is called the Hartree–Fock limit, E_{HF}, which corresponds to the best possible solution for the Schrödinger equation as there would not be any restriction for the electrons. [xv] Because an infinite set of atomic orbitals is impractical, a choice must be made on how to truncate the expansion. This choice of atomic orbitals defines the basis set (set of mathematical functions used to expand the molecular orbitals).[x,xvi]A natural starting point is to use functions (called basis functions: mathematical functions chosen to give the maximum flexibility to the molecular orbitals)[xvi] from the exact solution of the Schrödinger equation for the hydrogen atom. These orbitals have the form

$$\chi = Nx^i y^j z^k e^{-\zeta(r-R)}, \qquad (1.10)$$

where R is the position vector of the nucleus upon which the function is centred and N is the normalization constant. Functions of this type are called Slater-type orbitals (STOs). The construction of MOs in terms of some set of functions is entirely a mathematical "trick," these functions are placed at nuclei because that is the region of greatest electron density. "Atomic orbitals" are not used in the sense of a solution to the atomic Schrödinger equation, but just mathematical functions placed at nuclei for convenience, therefore it is common refer to the expansion of basis functions to form the MOs.[x]

Unfortunately, integration involving these STO functions can be difficult and they could be replaced by Gaussian functions (or Gaussian-type orbitals, GTOs), for which there exist analytical solution for the integrals.[vii] GTOs are not really orbitals. They are simpler functions, being a combination of functions used to mimic the STO that are frequently called gaussian primitives (usually obtained from quantum calculation on atoms)[xvii].These orbitals have the form

$$\chi = Nx^i y^j z^k e^{-\alpha(r-R)^2}, \qquad (1.11)^{x}$$

The shape of a Gaussian function is rather different from that of a Slater function, with the absence of a cusp at the nucleus and a more rapid drop in value with the distance from the nucleus (**Fig. 5**).[vii]

The minimum basis set has one basis function for every formally occupied or partially occupied orbital in the atom. So, the minimum basis set for carbon, with electron occupation $1s^2 2s^2 2p^2$, has two s-type functions and p_x, p_y, and p_z functions, for a total of five basis functions. This minimum basis set is referred to as a single-zeta (SZ) basis set. The use of the term zeta here reflects that each basis function mimics a single STO, which is defined by its exponent, z.[x] The most common minimal basis set is STO-nG,

where n is an integer. This n value represents the number GTOs used to approximate STO for both core and valence orbitals (**Fig. 6**).[xvii]

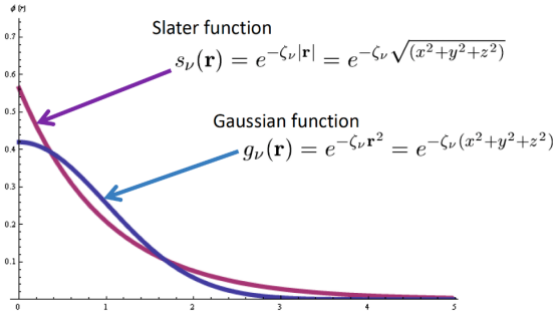

Figure 5. Radial component of a Slater-type orbital (STO) and a Gaussian-type orbital (GTO).[xviii]

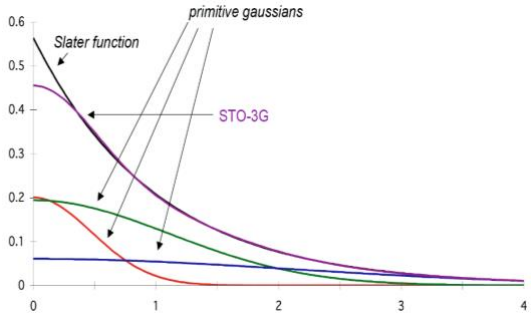

Figure 6. Formation of the basis set STO-3G by contraction of 3 Gaussian primitives.[xii]

The minimum basis set is usually inadequate, failing to allow the core electrons to get close enough to the nucleus and the valence electrons to delocalize. An obvious solution is to double the size of the basis set, creating a double-zeta (DZ) basis. So, for carbon, the DZ basis set has four s basis functions and two p basis functions (recognizing that the term “p basis functions” refers here to the full set of p_x, p_y, and p_z functions), for a total of ten basis functions. Further improvement can be had by choosing a triple zeta (TZ) or even larger basis set.[x]

As most of chemistry focuses on the action of the valence electrons, Pople developed the split-valence basis sets, which allow for size variations that occur in bonding, single zeta in the core and double zeta in the valence region.[x,xiv]

For the vast majority of basis sets, including the split-valence sets, the basis functions are not made up of a single Gaussian function. Rather, a group of Gaussian functions are contracted together to form a single basis function. The popular split-valence 6-31G basis specifies the contraction scheme employed. The dash separates the core (on the left) from the valence (on the right). In this case, each core basis function is comprised of six Gaussian functions. The valence space is split into two basis functions (VDZ), frequently referred to as the “inner” and “outer” functions. The inner basis function is composed of three contracted Gaussian functions, and each outer basis function is a single Gaussian function.[x]

Basis sets could be extended by including a set of functions, polarization functions, that mimic the atomic orbitals with angular momentum greater than in the valence space greatly improves the basis flexibility. They take into account the influence of the neighboring nuclei that distort (polarize) the electron density near a given nucleus.[xvi6]

The explicit indication of the number of polarization functions within parentheses is nowadays broadly used, *e.g.* 6-311G(2df,2p) means that two sets of d functions and a set of f functions added to nonhydrogen atoms and two sets of p functions added to the hydrogen atoms.

For anions or molecules with many adjacent lone pairs, the basis set must be augmented with diffuse functions to allow the electron density to expand into a larger volume.[x] For split-valence basis sets, this is designated by "+", as in 6-31+G(d). The existence of "++" indicates the addition of a set of diffuse s functions to hydrogen as long as the addition of a set of diffuse sp orbitals to the atoms in the first and second rows.[xvi] Usually the addition of polarization and diffuse functions to H atoms is not usually necessary.[vii]

Correlation-consistent basis sets were developed by Dunning. They were constructed to extract the maximum electron correlation energy for each atom. The correlation-consistent basis sets are designated as "cc-pVNZ," to be read as correlation-consistent polarized splitvalence N-zeta, where N designates the degree to which the valence space is split. As N increases, the number of polarization functions also increases. So, for example, the cc-pVDZ basis set for carbon is double-zeta in the valence space and includes a single set of d functions, and the cc-pVTZ basis set is triple-zeta in the valence space and has two sets of d functions and a set of f functions. The addition of diffuse functions to the correlation-consistent basis sets is designated with the prefix aug-, as in aug-cc-pVDZ.[x] Another example of basis set developed by Dunning is the designed to converge systematically to the complete basis set (CBS) limit using extrapolation techniques, which implies a bigger calculation than other widely used basis sets.[xvii]

3.6 Density Functional Theory (DFT)

Density functional theory (DFT) is a quantum mechanical theory used in physics and chemistry to investigate the electronic structure (principally the ground state) of many-body systems, in particular atoms, molecules, and the condensed phases.[xix]

The electronic wavefunction is dependent on 3n variables: the x, y, and z coordinates of each electron. The total electron density r(r), related to the probability of an electron being present at a specific location, is dependent on just three variables: the x, y, and z positions in space. Because r(r) is simpler than the wavefunction and is also observable, it might offer a more direct way to obtain the molecular energy.

The Hohenberg–Kohn existence theorem proves just that. There exists a unique *functional* such that

$$E[\rho(r)] = E_{elec}, \qquad (1.12)$$

where E_{elec} is the exact electronic energy being functional of the electron density. Furthermore, they demonstrated that the electron density obeys the variational theorem. This means that, given a specific electron density, its energy will be greater than or equal to the exact energy. These two theorems constitute the basis of density functional theory (DFT). The result is that evaluation of Eq. (1.12) might be easier than traditional ab initio methods because of the simpler variable dependence.

A mathematical function is one that relates a scalar quantity to another scalar quantity, that is, y= f(x). A mathematical *functional* relates a function to a scalar quantity and is denoted with brackets, that is, y=F[f(x)]. In Eq. (1.12), the function $\rho(r)$ depends on the spatial coordinates, and the electronic energy depends on the values (is a functional) of $\rho(r)$.

In order to solve for the energy via the DFT method, Kohn and Sham proposed that the functional has the form

$$E[\rho(r)] = T_{e'}[\rho(r)] + V_{ne}[\rho(r)] + V_{ee}[\rho(r)] + E_{xc}[\rho(r)] \qquad (1.13)$$

where V_{ne}, the nuclear-electron attraction term is

$$V_{ne}[\rho(r)] = \sum_{j}^{nuclei} \int \frac{Z_j}{|r - r_k|} \rho(r) dr, \qquad (1.14)$$

and V_{ee}, the classical electron-electron repulsion term, is

$$V_{ee}[\rho(r)] = \frac{1}{2} \int \int \frac{\rho(r_1)(r_2)}{|r_1 - r_2|} dr_1 dr_2. \qquad (1.15)$$

The real key, however, is the definition of the first term of Eq. (1.13). Kohn and Sham defined it as the kinetic energy of noninteracting electrons whose density is the same as the density of the real electrons, the true interacting electrons. The last term is called the exchange-correlation functional and is a catch-all term to account for all other aspects of the true system.

The Kohn–Sham procedure is then to solve for the orbitals that minimize the energy, which reduces to the set of pseudoeigenvalue equations

$$\hat{h}_i^{KS} \chi_i = \mathcal{E}_i \chi_i. \qquad (1.16)$$

This is closely analogous to the Hartree equations (Eq. 1.7). The Kohn–Sham orbitals are separable by definition (the electrons they describe are noninteracting), analogous to the HF MOs.[x] The procedure followed in the calculi using DFT is summarized in **Fig 7.**

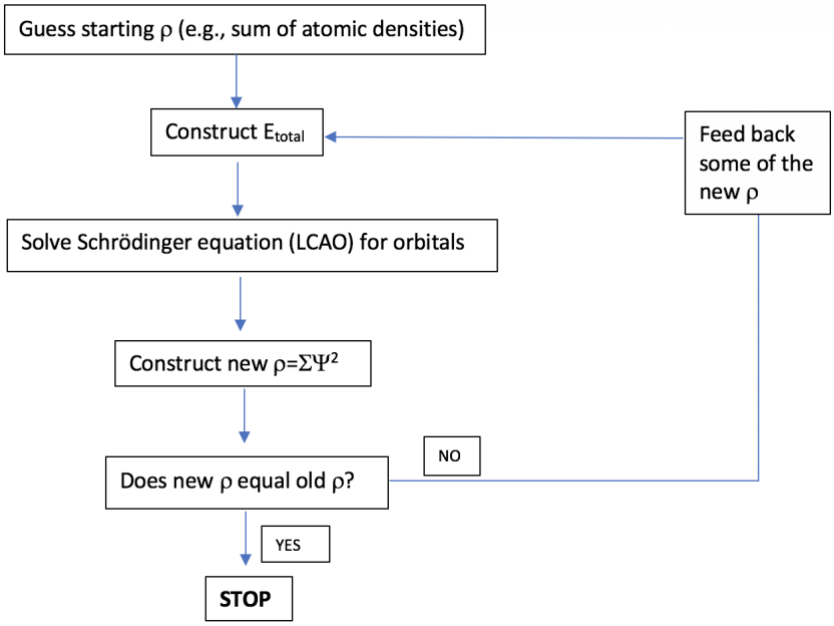

Figure 7. Flowchart for the different steps involved in the DFT procedure[xx]

DFT produces the energy of a molecule that includes the electron correlation for a similar computational cost as the HF method. DFT calculations are faster with better accuracy.[xxi] Although the Hohenberg–Kohn Theorem proves the existence of a functional that relates the electron density to the energy, it offers no guidance as to the form of that functional. The real problem is the exchange-correlation term. There is no way of deriving this term, and so a series of different functionals have been proposed, leading to many different DFT methods.[x]

Having its own pros and cons, DFT has become the most popular and versatile method in computational chemistry, accounting for approximately 90% of all calculations today.[xix]

3.6.1 Exchange-correlation functionals

The exchange-correlation functional is generally assumed as a sum of two components, an exchange part and a correlation part. These component functionals are usually written in terms of an energy density $\mathcal{E}$,

$$E_{xc}[\rho(r)] = E_x[\rho(r)] + E_c[\rho(r)] = \int \rho(r)\mathcal{E}_x[\rho(r)]dr + \int \rho(r)\mathcal{E}_c[\rho(r)]dr \qquad (1.17)$$

The DFT method is denoted with an acronym that defines the exchange functional and the correlation functional, in that order. For the exchange component, the most widely used is one proposed by Becke. It introduces a correction term to LSDA that involves the density derivative. The letter “B” signifies its use as the exchange term. Of the many correlation functionals, the two most widely used are due to Lee, Yang, and Parr (referred to as “LYP”) and Perdew and Wang (referred to as “PW91”). Last are the hybrid methods

that combine the exchange-correlation functionals with some admixture of the HF exchange term. The most widely used DFT method is the hybrid B3LYP functional, which includes Becke's exchange functional along with the LYP correlation functional:

$$E_{xc}^{B3LYP} = (1-a)E_x^{LSDA} + aE_x^{HF} + b\Delta E_x^B + (1-c)E_c^{LSDA} + cE_c^{LYP} \qquad (1.18)$$

The three variables (a, b, and c) are the origin of the "3" in the acronym. As these variables are fit to reproduce experimental data, B3LYP (and all other hybrid methods) contain some degree of "semi-empirical" nature. This has led to many discussions about how to classify DFT as it is not strictly ab initio.[x] It is common to find them discussed separately from ab initio and semi empirical methods in the literature. The accuracy of the electron density tends to increase along with the complexity of the density functional approximation.[xxii]

On average, there is considerable consensus that DFT methods are "better" than *ab initio* methods and are generally stated to be more accurate with lower computational expense.[xxi]

3.7 Geometry Optimization

The first step in performing a quantum chemical calculation is to select an appropriate method. The nomenclature for designating the method is "quantum mechanical treatment/basis set," such as MP2/6-31+G(d), which means that the energy is computed using the MP2 theory with the 6-31+G(d) basis set.

The general procedure in geometry optimization is to start with a guess of the molecular geometry and then systematically change the positions of the atoms in such a way as the energy decreases, continuing to vary the positions until the minimum energy is achieved, *i.e.* obtain the PES. Computation of all of the energy gradients with respect to the positions of the nuclei will offer guidance then in which directions to move the atoms. The second derivatives of the energy with respect to the atomic coordinates provides the curvature of the surface, which can be used to determine just how far each coordinate needs to be adjusted. The collection of these second derivatives is called the Hessian matrix, where each element H_{ij} is defined as

$$H_{ij} = \frac{\partial^2 E}{\partial q_1 q_2}, \qquad (1.19)$$

where q_i is an atomic coordinate (say for example the y-coordinate of the seventh atom). Efficient geometry optimization, therefore, typically requires the first and second derivatives of the energies with respect to the atomic coordinates. Computation of these

derivatives is always more time consuming than the evaluation of the energy itself. Further, analytical expression of the first and second energy derivatives is not available for some methods. An economical procedure is to evaluate the first derivatives and then make an educated guess at the second derivatives, which can be updated numerically as each new geometry is evaluated.[x]

The optimization procedure followed in many computational chemistry programs is depicted in **Fig. 8.**

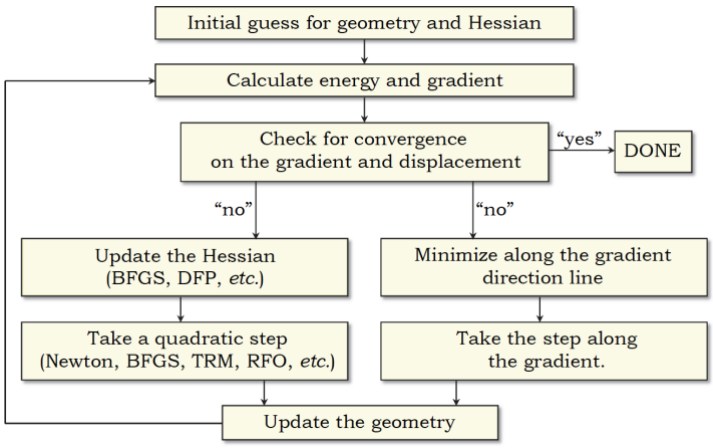

Figure 8. Flowchart for the different steps involved in the optimization procedure[xxiii]

The criteria for determining if a structure has been optimized is that any local energy minimum will have all of its gradients equal to zero. Typical practice is to set a small but nonzero value as the maximum acceptable gradient.

Testing of the gradient alone is not sufficient for defining a local energy minimum. Structures where the gradient vanishes are known as critical points, some of which may be local minima. The diagonal elements of the Hessian matrix, called its eigenvalues, identify the nature of the critical point. Six of these eigenvalues will have values near zero and correspond to the three translational and rotational degrees of freedom. If all of the remaining eigenvalues are positive, the structure is a local minimum. A transition state is characterized by having one and only one negative eigenvalue of the diagonal Hessian matrix. Computing the full and accurate Hessian matrix can therefore confirm the nature of the critical point, be it a local minimum, transition state, or some other higher-order saddle point. The Hessian matrix is useful in others ways, too. The square root of the element of the diagonal mass-weighted Hessian is proportional to the vibrational frequency ω_i. A relevant consequence is that any PES minima will show all vibrational frequencies positive. Within the harmonic oscillator approximation, the zero-point vibrational energy (ZPVE) is obtained as:

$$ZPVE = \sum_{i}^{vibrations} \frac{\hbar\omega_i}{2}. \qquad (1.20)$$

The vibrational frequencies can also be used to compute the entropy of the molecule and ultimately the Gibbs free energy.

The molecular geometry is less sensitive to computational method than is its energy. As geometry optimization can be computationally time-consuming, often a molecular structure is optimized using a smaller, lower-level method, and then the energy is computed with a more accurate higher-level method. For example, in this work geometry optimization was carried out at the DFT/6-31++G(d,p) level and then its corresponding energy using the B3LYP/aug-cc-pVTZ method. This computation is designated "DFTB3LYP/aug-cc-pVTZ//DFT/6-31++G(d,p)" with the double slashes separating the method used for the single-point energy calculation (on the left-hand side) from the method used to optimize the geometry (on the right-hand side).[x]

3.8 Solvation Models

Solvation is defined by the IUPAC as "any stabilizing interaction of a solute (or solute moiety) and the solvent or a similar interaction of solvent with groups of an insoluble material",[xxiv] and a solvent is a substance that dissolves a solute, resulting in a solution. We can have Solvents can be classified as:

- Polar solvents. We can distinguish 2 groups of polar solvents:
  a) Protic polar solvents: contain (a) labile proton(s)
  b) Aprotic polar solvents: cannot donate protons
- Non-polar solvents.[xxv]

Solvation can alter the properties of a molecule, e. g. its charge distribution, geometry, vibrational frequencies, electronic transition energies, NMR constants, chemical reactivity, etc. Of particular interest for thermodynamic considerations is the solvation free energy, which is the net energy change upon transferring the molecule from the gas phase into a solvent with which it equilibrates.

Efficient simplified models can implicitly treat the various physical influences of solvent molecules on the solute. These influences are often phenomenologically classified as electrostatic (including induction), cavitation, exchange repulsion, and dispersion attraction. For a polar solute in a polar solvent the electrostatic interactions (including induction) are usually dominant, but the other effects noted above still need to be included for quantitative work. The electrostatic interaction is long range and can be

understood classically, while the others are short range and inherently quantum mechanical in origin.[xxvi]

In summary, three solvation effects can be taken into account:

1. Non-specific static interactions: polarization, dipole orientation, quadrupole orientation…
2. Specific static interactions: hydrogen bonds, Van der Waals interaction, charge transfer effects.
3. Thermodynamic and statistical effects: hydrophobic effect, solvation shell structure.[xxvii]

And three solvation models can be considered:

1. Explicit models: include molecular details of each solvent molecule.
2. Implicit models: treat solvent as a continuous system
3. Hybrid models: consider first (and second) solvation sphere explicitly while the rest of the solvent is treated in implicit way.

Here, we will focus on the implicit ones.

3.8.1 Implicit models

In the implicit models, the solvent is a uniform, polarizable medium with fixed dielectric constant while the solute is placed inside the cavity in the medium. Those models differ in the following aspects:

1. Size and shape of the molecular cavity in which the solute is accommodated: spherical, ellipsoidal, Van der Waals spheres …
2. Level of solute description: classical molecular mechanics, semi-empirical quantum mechanics, *ab initio*, DFT…
3. Dielectric medium description: in most cases a homogeneous static medium with fixed dielectric constant is stated.
4. The cavity calculation method and representation of charge distribution:[xxv] for their description, we will focus in the Polarizable Continuum Model (PCM).

3.8.2 Polarizable Continuum Model (PCM)

The following issues should be highlighted for this model:

- The cavity is defined by overlapping Van der Waals spheres, having an isodensity surface which is solvent-accessible (SAS).

- The electrostatic potential from solute and polarization of solvent must obey the Poisson equation.
- Electrostatic interactions are calculated numerically.
- There are different formulations: SMD, DPCM, IPCM, SCIPCM, IEFPCM…[xxv,xxviii]

3.8.3 Solvation Model based on Density (SMD)

A widely used PCM model is the universal implicit solvent model called Solvation Model based on Density (SMD), where "universal" denotes its applicability to any charged or uncharged solute in any solvent or liquid medium for which a few key descriptors are known (e.g. the dielectric constant). The SMD model is based on the quantum mechanical charge density of a solute molecule interacting with a continuum description of the solvent. In this model, solvent accessible surface (SAS) encloses a superposition of nuclear-centered spheres. The SMD model achieves mean unsigned errors of 2.4 - 4.0 kJ/mol in solvation free energies of tested neutrals and mean unsigned errors of 25 kJ/mol on average for ions, whereas other default solvation methods have unsigned errors of 4-25 kJ/mol for these neutrals and 30 -42 kJ/mol for ions.[xxix]

4. MATERIALS AND METHODS

4.1 Hardware and Software

4.1.1 Hardware

Electronic structure calculations were performed in the supercomputer Finis Terrae II, located at the "Centro de Supercomputación de Galicia" (CESGA). The main characteristic of FT2 are the following: the Finis Terrae II supercomputer (FT-II) is a computing system based on Intel Haswell processors and interconnected by Infiniband network with a peak performance of 328 TFlops and sustained in Linpack of 213 Tflops. It is composed of 3 types of computing nodes, the 306 compute nodes "Thin" each having to be highlighted with: 2 Haswell 2680v3 processors, 24 cores; 128 GB memory; 1 disc of 1TB; 2 connections 1GbE; 1 Infiniband FDR @ 56Gbps connection. It has a parallel file system Lustre with 768TB of capacity (750TB net) and 20GB / s of read / write, being its total consumption of 118Kw and peak performance of 328 TFlops (240 Tflops Linpack). The FT-II supercomputer has a high performance Mellanox Infiniband FDR @ 56 Gbps interconnection network with Fat-tree topology.[xxx]

4.1.2 Software

The programs/applications used in this project were the following:

- Word processor: Word 2016 for Mac OSX.
- Data analysis and graphing software: Excel 2016 for Mac OSX and Origin 8.0 for windows. [xxxi]
- Supercomputer connection: FortiClient (version 5.6 for Max OSX)
- Files transfer: SSH Secure Shell Client (version 3.2.9 for Windows), WinSCP (version 5.13 for Windows)
- Electronic structure calculations: Gaussian09 (for Windows), Gaussian16 (for Windows).[xxxii]
- Molecular visualization: GaussView (version 6.0 for Windows),[xxxii] GabeEdit (version 2.1.0 for Windows) and Mercury (version 3.10.2 for Windows).
- Chemical drawing: ChemDraw05.[xxxiii]
- Bibliographic manager: RefWorks.

An example of input file and as long as the way the information can be taken from the output file for geometry optimization used in this work appear in **Annex 1a & 1.b.**

4.2 Model Chemistry

Electronic structure calculations were carried out with the Gaussian09 package for benzoic acid and Gaussian16 package for phthalic and carborane dicarboxylic acids and

H_2O and H_3O^+ molecules. The selected theoretical method was DFT with the B3LYP functional and basis set 6-31++G(d,p) for the carboranes dicarboxylic acids, which is of double-ζ quality, with polarization and diffuse functions for all atoms. The basis set 6-31+G(d,p), with polarization functions for all atoms and diffuse functions for boron and carbon, was used for benzoic acid as well as for phthalic acids.

The thermochemistry of studied species was computed as the contribution of the electronic energy -nuclear repulsion included- (E_{el}), the zero-point vibrational energy (ZPE) and the computed thermal energy, enthalpy and Gibbs free energy change from 0K to the working temperature (298.15K) ($\Delta G° \rightarrow$ 298.15K), *i.e.*:

$$G^o_{(g\ or\ aq)} = E_{el} + ZPE + G^o_{0\,K \rightarrow TK} \qquad (2.1)$$

where E_{el} is the electronic energy (including nuclear repulsion), ZPE is the zero-point vibrational energy, $\Delta G_{0 \rightarrow 298K}$ is the calculated thermal free energy change going from 0K to the working temperature, the degree symbol (°) denotes the gas phase standard state. E_{el} was obtained for neutral molecules, monoanions and dianions in the gas phase performing an optimization calculation on the previously optimized structures of the corresponding conformational study. RHF calculations were carried out for all closed shell species, whereas UHF calculations were used for open shell ones.

Improvement of electronic energy was obtained by single point calculations using the aug-cc-pVTZ basis set, *i.e.*, DFT/aug-cc-pVTZ //B3LYP/6-31++G(d,p) calculations.

The SMD implicit solvation model was chosen to simulate water as a solvent, *i.e.* SMD/B3LYP/6-31++G(d,p) level of calculation. Gaussian16 package default values were used.

4.3 Calculation of Acid Dissociation Equilibria

Acid dissociation constants, also known as pK_a values, are essential for understanding many fundamental reactions in chemistry and biochemistry. For a weak acid dissociation:

$$HA_{(aq)} \leftrightharpoons A^-_{(aq)} + H^+_{(aq)} \qquad (2.2a)$$

or

$$HA_{(aq)} + H_2O(l) \leftrightharpoons A^-_{(aq)} + H_3O^+_{(aq)} \qquad (2.2b)$$

pK_a is defined as for Eq. 2.2a:

$$pK_a = -logK_a \qquad (2.3)$$

$$K_a = \frac{\left[A^-_{(aq)}\right]_{eq}\left[H^+_{(aq)}\right]_{eq}}{\left[HA_{(aq)}\right]_{eq}} \qquad (2.4)^{xxxiv}$$

This equilibrium constant can be also calculated, at a given temperature and pressure, in terms of the Gibbs free energy (hereafter denoted as free energy):

$$K_a = e^{-\frac{\Delta G^*_{rxn}}{R\cdot T}} = e^{-\frac{G^*_{A^-(aq)}+G^*_{H^+(aq)}-G^*_{HA(aq)}}{R\cdot T}} \qquad (2.5)$$

where R is the universal gas constant, T the temperature in the Kelvin scale and the asterisk (*) denotes, using Ben-Naim and Marcus notation, the solution standard state.[xxxv] From Eq. 2.5 it follows:

$$pK_a = -\log K_a = \frac{\Delta G^*_{rxn}}{\log(10)\cdot R\cdot T} = \frac{G^*_{A^-(aq)} + G^*_{H^+(aq)} - G^*_{HA(aq)}}{2.303\cdot R\cdot T} \qquad (2.6)$$

Often pK_a values can be measured quite easily; however, chemists are sometimes interested in pKa values of molecules that have not been synthesized or for which experiments are not straightforward. Thus, computational chemistry plays an important role in pK_a calculations where it is hard to achieve an accurate result. Calculation of acid dissociation constants using Computational Chemistry is a demanding and arduous process because an error of *ca.* 6 kJ/mol in the change of free energy of reaction (1) results in an error of one pKa unit. There are numerous studies that use a variety of methods in an attempt to obtain this chemical accuracy. In recent years, there have been new developments, but many discrepancies still exist.[xxxiv]

In this work six different methods of pK_a calculation have been tested, some of them using thermodynamic cycles. In all cases temperature was fixed at 25ºC, *i.e.* 298.15K, and one atm for pressure and one mol·dm^{-3} as standard states for the gas phase and aqueous solution, respectively.

4.3.1 *Method 1. Thermodynamic cycle involving gas phase and aqueous solution calculations using chemical equilibrium 2.2a.*

The chemical equilibrium described in Eq. (2.2a) has been used, and the corresponding pK_a values have been calculated using the thermodynamic cycle shown in **Fig. 9.**

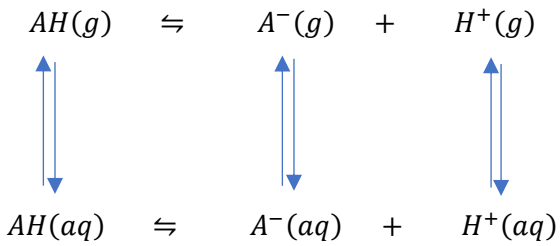

Figure 9. Thermodynamic cycle for calculation of pK_as as a mixture of gas phase-solution species within a proton-based point of view.

This is one of the most common methods used. In this case, pK_a is obtained following the strategy of Psciuk *et al.,* as a combination of gas phase-solution calculations.[xxxv] Starting from the gas phase contribution, the change in gas phase Gibbs free energy (ΔG_{gas}) is calculated as the contribution of the electronic energy of each specie, at 0 K, the zero-point energy and thermal corrections (0 → 298.15K), see Eq. (2.1).

For the gas phase:

$$\Delta G_{gas} = G^0_{A^-(g)} + G^0_{H^+(g)} - G^0_{AH(g)}$$

The next step is to calculate the change in solvation free energy (ΔG_{solv}):

$$\Delta G_{solv} = \Delta G_{solvA^-} + \Delta G_{solvH^+} - \Delta G_{solvAH}$$

Solvation free energies are obtained subtracting the electronic energy in the gas phase directly to the electronic energy in aqueous phase:

$$\Delta G_{solvAH} \approx E_{el,AH(aq)} - E_{el,AH(g)}$$

$$\Delta G_{solvA^-} \approx E_{el,A^-(aq)} - E_{el,A^-(g)}$$[xxxvi]

All of these free energy values can be calculated using quantum chemistry, except $\Delta G_{solv}(H^+)$ and $G^0_{gas}(H^+)$, which must be determined experimentally or using thermodynamic theory, as $H^+(g)$ has no electrons.[xxxiv]

For pK_a computations in solution, the absolute free energy of the solvated proton is a critical parameter, usually computed as the contribution of the absolute free energy of the proton in the gas-phase at standard temperature and pressure (-26,28 $KJ \cdot mol^{-1}$ at 298,15 K), which is obtained with the Sackur-Tetrode equation, and the Gibbs energy of proton solvation in water.[xxxvi] A value of -265.9 kcal/mol for this last one will be taken.

According to the literature this value is accepted as the closer to the real one.[xxxiv] The conversion from gas-phase standard state (1 atm) to solution standard state (mol·dm^{-3}) is taken into account by adding 1.89 kcal/mol to the calculation.[xxxv,xxxv] So, ΔG_{solvH+} value was calculated as:

$$\Delta G_{solvH^+} = -26.28\frac{kJ}{mol} + \left(-\frac{265.9\ kcal}{mol} + 1.89\frac{kcal}{mol}\right) \cdot 4.184\frac{kJ}{1Kcal} = 1130.9\frac{kJ}{mol}$$

$$\Delta G_{solvH^+} = 1130.9\frac{kJ}{mol}$$

Therefore, ΔG_{Total} is:

$$\Delta G_{Total} = \Delta G_{gas} + \Delta G_{solv}$$

Finally, pK_a calculation can be done using Eq. (2.6).

4.3.2 *Method 2. Direct method using calculated Gibbs free energies in solution for the chemical equilibrium 2.2a*

An alternative way for the computation of pK_a is considering the Gibbs free energy of the optimized structures in solution of the neutral species and of the anion (Eq. 2.2a) together with the proton solvation free energy –calculated as in method 1–, and then use Eq. 2.6 to obtain the acidity constant.

4.3.3 *Method 3. Isodesmic method*

Calculated acidity constants are estimated with respect to the pK_a of a reference acid:

$$HBz\ (aq) + A^-(aq) \leftrightharpoons AH(aq) + Bz^-(aq)$$

In this thermodynamic cycle benzoic acid was taken as reference. ΔG_{Total} is obtained as:

$$\Delta G_{Total} = G_{AH(aq)} + G_{Bz^-(aq)} - G_{HBz(aq)} - G_{A^-(aq)}$$

And the pK_a of interest calculated as:

$$pK_a = pK_{aBz} - \Delta pK_a$$ [xxxvii]

Error cancellations lead to minimize systematic errors in the pK_a prediction.

4.3.4 *Method 4. Direct method using calculated Gibbs free energies in solution for the chemical equilibrium 2.2b*

ΔG_{Total} is calculated from the free energy of the species involved in Eq. 2.2b:

$$\Delta G_{Total} = G_{A^-(aq)} + G_{H_3O^+(aq)} - G_{AH(aq)} - G_{H_2O}(l)$$

This time the logarithm of water molarity (55.56) should be subtracted to obtain consistent pK_a values, as this constant concentration is not included in the right term of Eq. (2.4).

4.3.5 *Method 5. Thermodynamic cycle involving gas phase and aqueous solution calculations using chemical equilibrium 2.2b*

This time the thermodynamic cycle shown in **Fig. 10** was used.

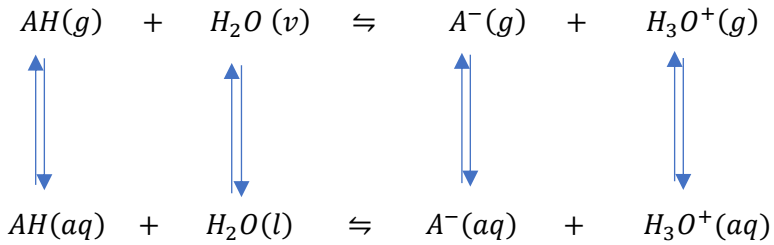

Figure 10. Thermodynamic cycle for calculation of pK_as as a mixture of gas phase-solution species adding explicit molecules of water

As before, the calculation of the different terms was analogous to that of Method 1, subtracting as well, the logarithm of the water molarity.

4.3.6 *Method 6. Thermodynamic cycle involving gas phase and aqueous solution calculations, using empirical solvation free energy values for H_2O and H_3O^+, in chemical equilibrium 2.2b.*

Calculation of pK_a values is similar to method 5 except solvation free energy for H_2O and H_3O^+. Here -26.44 and -461.08 $kJ \cdot mol^{-1}$ [xxxvii] were used for water and hydronium ion, respectively.[xxxviii]

4.4 *Calculation of Redox Potentials*

The absolute monoelectronic reduction potential $-E^0_{red(sol)}-$ of a specie, namely $B^{\cdot+}$, in a given solvent can be described by the following chemical equation:

$$B^{\cdot+}(sol) \quad + \quad e^-(g) \quad \rightarrow \quad B(sol)$$

It can be calculated in terms of Gibbs free energy as:

$$E^{\circ}_{red(sol)} = \frac{-\Delta G^*_{red(sol)}}{F} \qquad (2.7)$$

where F is the Faraday's constant and, $\Delta G^*_{red(sol)}$ is the solution phase standard state free energy change. Practical reasons impede the direct determination of absolute redox potentials; therefore, they are measured against a reference electrode and are reported as relative half-cell potentials. For comparison with experimental results, the absolute

potential of the standard hydrogen electrode in an aqueous solution [E^0(SHE) = 4.281 V] has been taken as a reference.[xxxv]

Two methods have been used to calculate monoelectronic reduction potentials, one of them through a thermodynamic cycle. As before, temperature was fixed at 25°C. *i.e.* 298.15 K, and one atm for pressure and one mol·dm^{-3} as standard states for the gas phase and aqueous solution respectively.

4.4.1 *Method 1. Thermodynamic cycle involving gas phase and aqueous solution calculations*

Fig. 11 shows the thermodynamic cycle used to compute $\Delta G^*_{red(sol)}$.

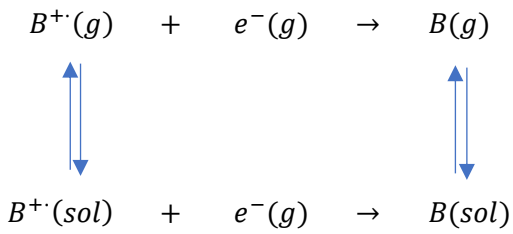

Figure 11. Thermodynamic cycle for calculation of the absolute one-electron reduction potential in solution.

Using the thermodynamic cycle outlined in **Fig. 11**, $\Delta G^*_{red(sol)}$ is calculated as:

$$\Delta G^*_{red(sol)} = G^*_{(sol)}(B) - G^*_{(sol)}(B^{+\cdot}) - G^{\circ}_{(g)}(e^-) \qquad (2.8)$$

where $G^*_{(sol)}$ is obtained as:

$$G^*_{(sol)} = \left(G^{\circ}_{(g)} + \Delta G^{1atm \rightarrow 1M}\right) + \Delta G^*_{solv} \qquad (2.9)$$

where $\Delta G^{\circ}_{(g)}$ is the standard state free energy in the gas phase and ΔG^*_{solv} is the standard state free energy of solvation. $\Delta G^{1atm \rightarrow 1M}$ is the free energy difference accounting for the standard state change from the gas phase to solution. Substituting equation 2.9 into 2.8 yields $\Delta G^*_{red(solv)}$:

$$\Delta G^*_{red(sol)} = (G^{\circ}_{(g)}(B) + \Delta G^{1atm \rightarrow 1M} + \Delta G^*_{solv}(B)) - (G^{\circ}_{(g)}(B^{+\cdot}) + G^{\circ}_{(g)}(e^-) + \Delta G^{1atm \rightarrow 1M} + \Delta G^*_{solv}(B^{+\cdot})) \qquad (2.10)^{xxxv}$$

Solvation free energy for each chemical species was obtained similarly to method 1 of pKa calculation, and one-electron reduction potential estimated using Eq. 2.7.

4.4.2 *Method 2. Direct method using calculated Gibbs free energies in solution*

An alternative way for the computation of the redox potentials is by using the Gibbs energy of the optimized structures of the species in solution. In this case $\Delta G^*_{red(sol)}$ is obtained as:

$$\Delta G^*_{red(sol)} = G^*_{(sol)}(B) - G^*_{(sol)}(B^{+\cdot}) - G^*_{(g)}e^-$$

and the one-electron reduction potential is to be calculated using Eq. 2.7.

5. ***WORK PLAN***

The activities developed during this Bachelor final degree dissertation were chronological carried out as follows in the following chronogram:

Table 3. Summary of the project's work plan

	FEBRUARY				**MARCH**				**APRIL**				**MAY**				**JUNE**			
Months divided in four weeks	**1**	**2**	**3**	**4**	**1**	**2**	**3**	**4**	**1**	**2**	**3**	**4**	**1**	**2**	**3**	**4**	**1**	**2**	**3**	**4**
Connection to CESGA		X																		
Use of molecular calculation and visualization programs		X	X	X																
Bibliographic search (Web of Science) and readings							X	X	X	X	X	X	X	X	X	X	X	X	X	
Use of bibliographic manager		X																		
Learning fundamentals of Computational Chemistry							X	X	X	X	X	X	X	X						
Deepening on *Ab initio* and DFT methods										X	X	X	X	X						
Optimization of molecular geometry		X	X	X	X	X	X	X	X	X	X	X	X	X	X	X	X	X	X	
Determination of acidity constants and redox potentials													X	X	X	X	X	X	X	
Analysis of results																	X	X	X	
Memory writing							X	X	X	X	X	X	X	X	X	X	X	X	X	

6. RESULTS AND DISCUSSION

The following systems have been studied:

Name	Chemical formula	IUPAC name	CAS Number[xxxix]	EC Number[xl]
Benzoic acid	$C_7H_6O_2$	Benzenecarboxylic acid	65-85-0	200-618-2
Phthalic acid	$C_8H_6O_4$	1,2-Benzenedicarboxylic acid	88-99-3	201-873-2
Isophthalic acid	$C_8H_6O_4$	1,3- Benzenedicarboxylic acid	121-91-5	204-506-4
Terephthalic acid	$C_8H_6O_4$	1,4- Benzenedicarboxylic acid	100-21-0	202-830-0
o- Carborane dicarboxylic acid	$C_4H_{12}B_{10}O_4$ $C_2B_{10}H_{10}(CO_2H)_2$	1,2-closo-dicarbadodecaborane-1,2-dicarboxylic acid	16872-09-6	240-897-8
m- Carborane dicarboxylic acid	$C_4H_{12}B_{10}O_4$ $C_2B_{10}H_{10}(CO_2H)_2$	1,7-closo-dicarbadodecaborane-1,7-dicarboxylic acid	16986-24-6	241-065-7
p- Carborane dicarboxylic acid	$C_4H_{12}B_{10}O_4$ $C_2B_{10}H_{10}(CO_2H)_2$	1,12-closo-dicarbadodecaborane-1,12-dicarboxylic acid	20644-12-6	-

The studied compounds are dicarboxylic acids. In a general way their acid-base equilibria can be described as shown in **Fig. 12**.

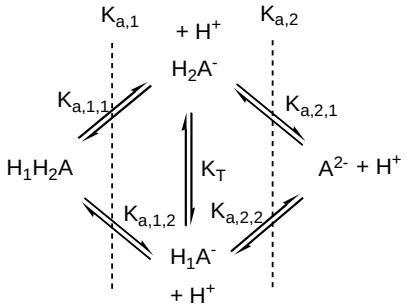

Figure 12. Microscopic ($K_{a,1,1}$, $K_{a,1,2}$, $K_{a,2,1}$ & $K_{a,2,2}$) and macroscopic ($K_{a,1}$ & $K_{a,2}$) equilibria of a general dicarboxylic acid H_1H_2A.

Considering the nature of the dicarboxylic acids studied here, it follows that monoanions H_1A^- and H_2A^- are indistinguishable, which simplifies the calculation (**Fig. 13**), but such statistical contribution should be taken into account (see **Annex 3**).

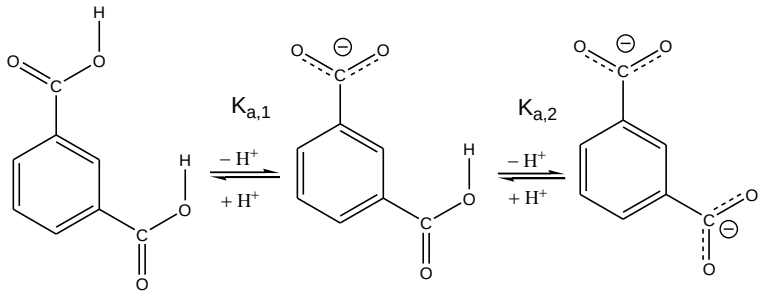

Figure 13. Acid base equilibria (K_{a1} & K_{a2}) under study of the isophthalic acid

Atom numbering used in this work is shown in **Fig 14**. Isophthalic acid has been selected as an example. The same applies for the other dicarboxylic acids. Subscript 1 was assigned to carboxyl group that loses the acidic hydrogen in the first equilibrium (pK_{a1}), and subscript 2 for the second deprotonation (pK_{a2}).

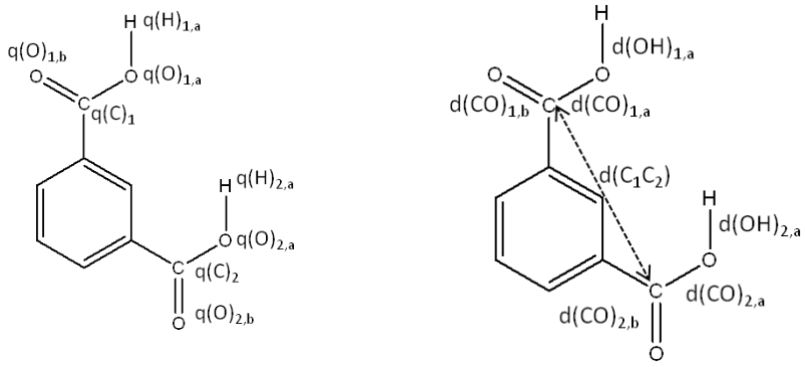

Figure 14. Atom numbering for the he carboxyl groups for the dicarboxylic acids.

6.1 Conformational Studies

6.1.1 Benzoic acid

Benzoic acid has been chosen as a reference in the isodesmic method. Its geometry was optimized at the B3LYP/6-31+G(d,p) level of theory in the gas phase and using the SMD/B3LYP/6-31+G(d,p) level of theory in water. Then, a PES was obtained rotating the carboxyl group 360° (taking 30° each rotation). The obtained PES is depicted in **Fig. 15.** There are two minima corresponding to the structures in which the carboxyl group is coplanar to the benzene ring.

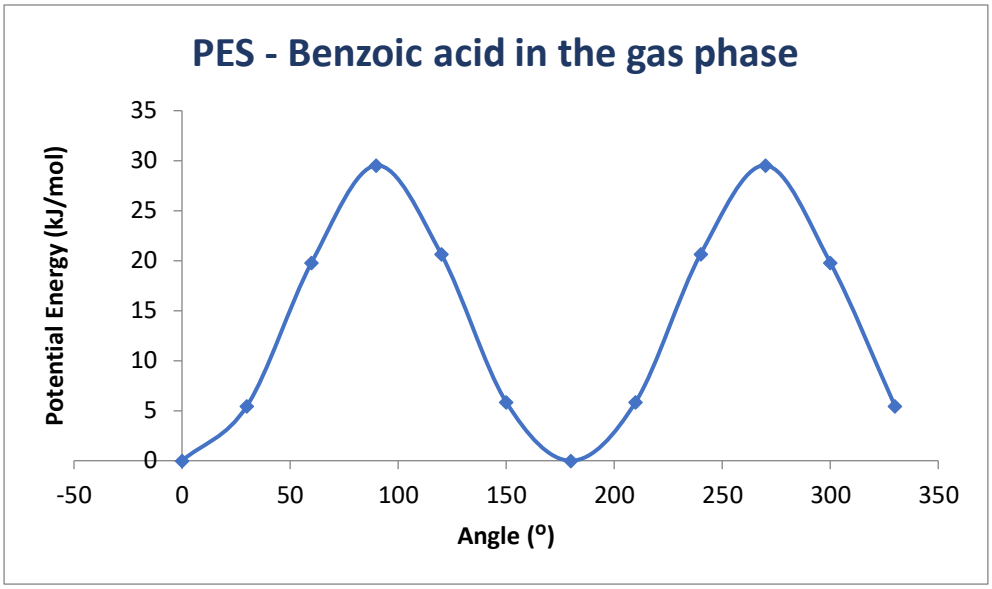

Figure 15. 2D-PES of benzoic acid in the gas phase at the B3LYP/6-31+G(d,p) level of theory .

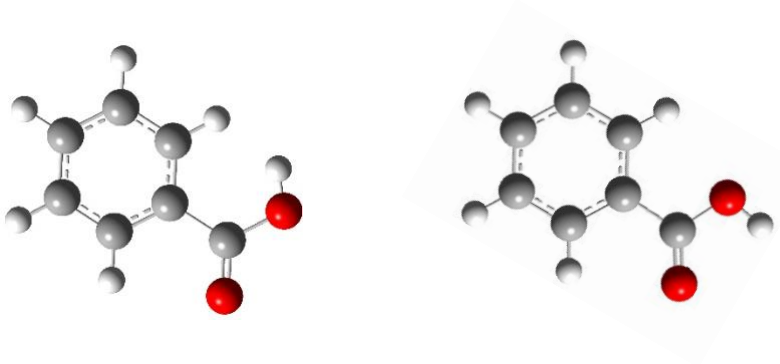

Figure 16. Minimum energy conformation for the acidic hydrogen of benzoic acid.

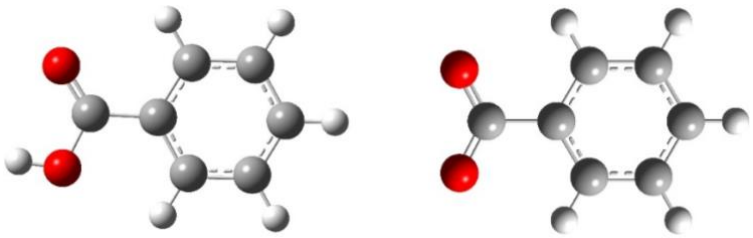

Figure 17. Optimized structures of benzoic acid and benzoate anion in water at the SMD/B3LYP/6-31+G(d,p) level of theory.

Studies on different orientations of the hydrogen bonded to the oxygen were also performed (**Fig. 16).** The difference between those conformations was 30.4 kJ/mol, being more stable the one placed at the right. This structure was used for subsequent calculations. The chosen structure and the corresponding benzoate anion were optimized in the gas phase and in water. The most stable structures obtained in water are shown in **Fig. 17.**

6.1.2 *Carborane dicarboxylic acids*

The geometry of the carborane dicarboxylic acids was optimized at the B3LYP/6-31++G(d,p) level of theory in the gas phase and using the SMD/B3LYP/6-31++G(d,p) level of theory for optimizations in water. Then, a PES was obtained rotating both carboxylate groups 360° (taking 30° each rotation). 3D potential energy surfaces were obtained, having all of them a shape similar to that shown in **Fig. 18.**

In this case, the minima search was more complex, being more hard-working to find it than in the case of the benzoic acid. Minima were determined using the Excel 2016 program, a typical table is shown in **Table 4.**

The most stable structures of the carboranes dicarboxylic acids were then optimized at the B3LYP/6-31++G(d,p) level of theory for optimizations in the gas phase and using the SMD/B3LYP/6-31++G(d,p) level of theory for optimizations in water. **Fig. 19** shows the most stable structures obtained for the carborane dicarboxylic acids (neutral, monoanion and dianion) in water after conformational search.

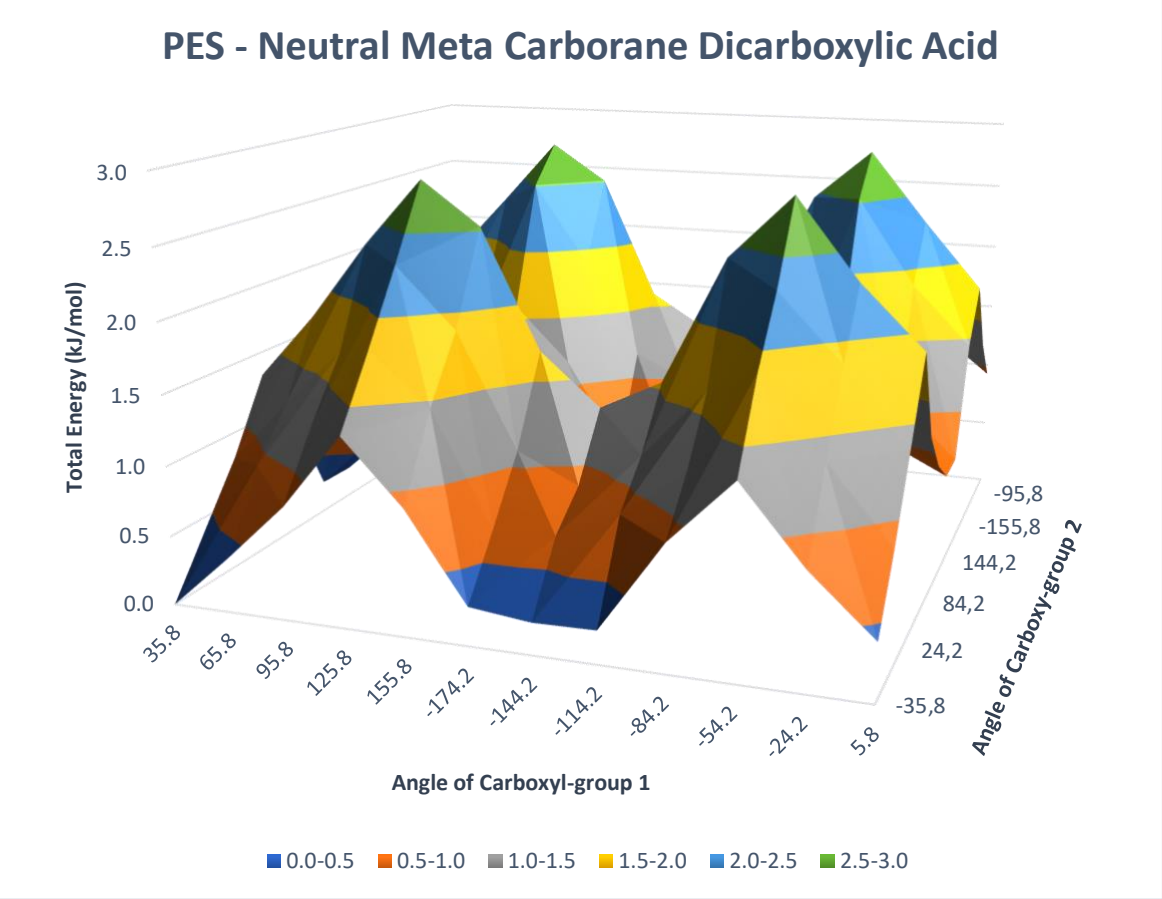

Figure 18. 3D-PES for *meta*-carborane dicarboxylic acid at the B3LYP/6-31++G(d,p) level of theory

Table 4. Search of the lowest energy conformational for *meta*-carborane dicarboxylic acid. Green: minimum; orange: maximum.

		Rotation of carboxyl group 1 / º											
		35.8	65.8	95.8	125.8	155.8	-174.2	-144.2	-114.2	-84.2	-54.2	-24.2	5.8
Rotation of carboxyl group 2 / º	-35.8	***0.0***	0.4	0.8	1.3	0.9	0.3	0.2	0.2	0.9	1.3	0.8	0.4
	-5.8	0.4	0.9	1.3	1.8	1.5	0.7	0.7	0.9	1.2	1.9	1.4	0.9
	24.2	0.8	1.3	1.7	2.3	1.9	1.1	0.9	1.1	1.6	2.3	1.9	1.4
	54.2	1.3	1.8	2.4	2.8	2.5	1.7	1.3	1.5	2.4	2.9	2.3	1.9
	84.2	0.9	1.4	1.8	2.5	1.6	1.1	1.0	1.1	1.7	2.4	1.6	1.2
	114.2	0.2	0.6	1.0	1.6	1.1	0.8	0.5	0.4	1.1	1.5	1.1	0.9
	144.2	0.2	0.7	0.9	1.3	1.0	0.5	0.4	0.5	1.0	1.3	0.9	0.7
	174.2	0.3	0.9	1.1	1.6	1.2	0.5	0.5	0.8	1.1	1.7	1.1	0.7
	-155.8	0.9	1.2	1.6	2.5	1.9	1.2	1.0	1.1	1.6	2.5	1.9	1.5
	-125.8	1.3	1.9	2.3	2.8	2.5	1.6	1.3	1.6	2.5	2.8	2.3	1.8
	-95.8	0.8	1.3	1.8	2.3	1.6	1.2	0.9	1.0	1.8	2.4	1.7	1.3
	-65.8	0.4	0.8	1.3	1.9	1.2	0.9	0.7	0.6	1.3	1.8	1.3	0.9

The so-obtained geometric parameters of the studied carborane dicarboxylic acids in water solution are collected in **Table 5.** Comparing separately the neutral, monoanion and dianion geometric parameters for the different positional isomers, in water solution, if follows that the values for them are similar. An exception being the angle between carboxyl-groups, and, obviously, the d(C_1-C_2) value, *i.e.* the carboxyl-groups distance. The angle between carboxyl groups is almost orthogonal in *o*- and *p*-isomers, whereas becomes almost coplanar for *m*-isomer. A similar trend is observed for the monoanion. This angle decreases for the dianion of *o*- and *p*-isomers; whereas clearly the coplanarity is lost in the *m*-isomer.

The values for the *para*-monoanion must be treated carefully as the optimization in water failed. Values in **Table 5** correspond to the gas phase assuming similar geometry change in going from the gas phase to solution.

B-B, B-C and B-H distances are given with only 2 significant figures as they represent average values. The obtained values are almost identical regardless the chemical species.

The results obtained for the $(CO)_{a,1}$, $(CO)_{b,1}$, $(CO)_{a,2}$ and $(CO)_{b,2}$, distances demonstrate that for the neutral molecules $(CO)_{a,1}$ and $(CO)_{b,1}$ distances have different values that changed after the first deprotonation, turning into similar values for the monoanion. Once the carboxyl-group loses the acidic hydrogen, it is stabilized by resonance, and both C-O bonds become identical, likely with a bond order *ca.* 1.5. The same was obtained for the $(CO)_{a,2}$ and $(CO)_{b,2}$ distances regarding to the second deprotonation.

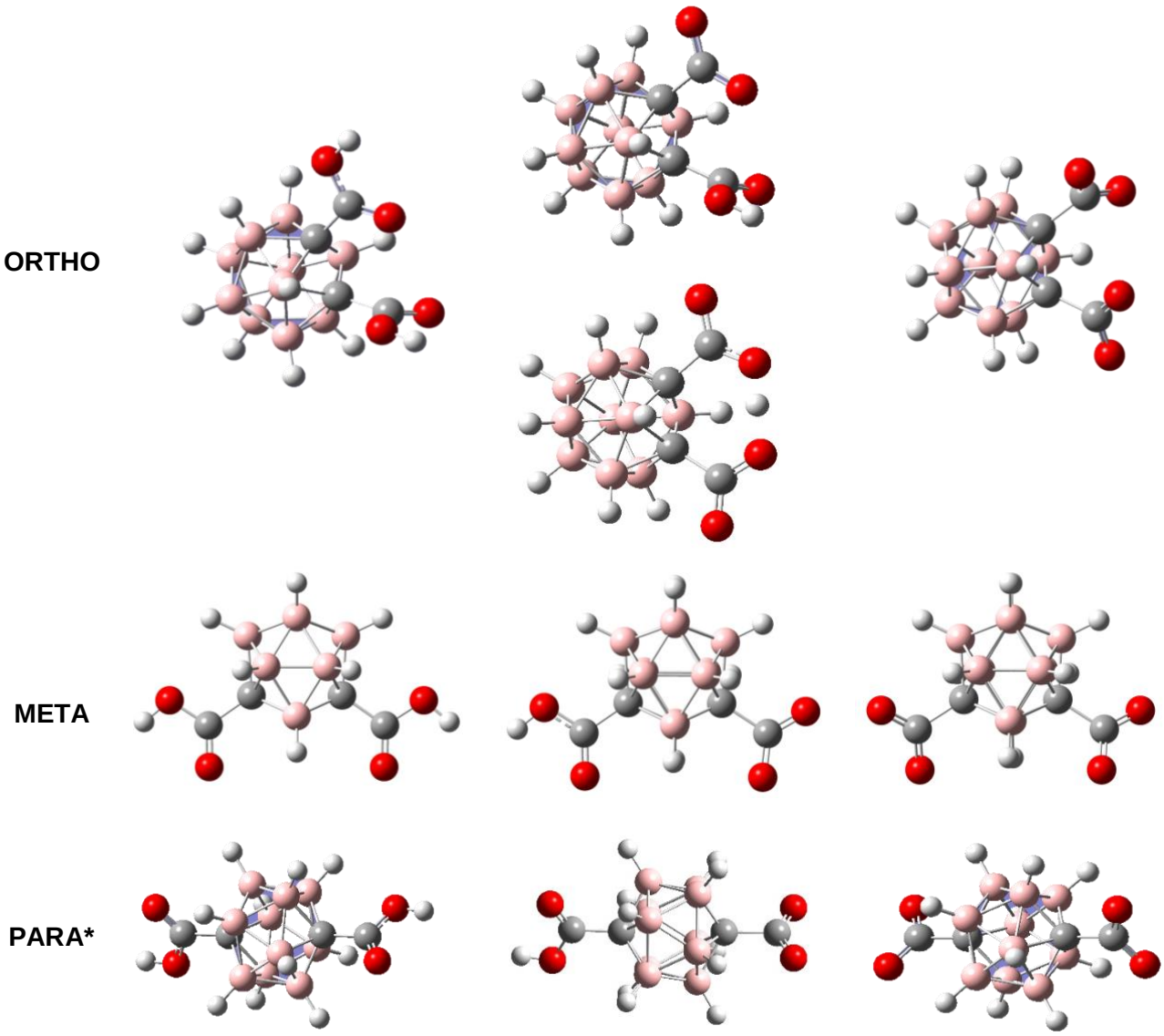

Figure 19. Optimized structures for *ortho-, meta-* and *para-* isomers of carborane dicarboxylic acids in water at the SMD/B3LYP/6-31++G(d,p) level of theory. * *p*-monoanion optimized structure in the gas phase.

For the neutral *ortho*-isomer, the formation of an intramolecular hydrogen bond is not favorable, whereas it is for *ortho*-monoanion. The difference in the Gibbs free energy for the *ortho*- monoanion isomer in water is in favor of the intramolecular H-bonded anion by 23.4 $kJ \cdot mol^{-1}$. The changes in the geometry of the optimized *ortho*-monoanion mainly have to do with carboxyl and carboxylate groups (**Table 5**), both in the same plane.

Table 5. Geometric parameters of carboranes dicarboxylic acids in water. SMD/B3LYP/6-31++G(d,p) level of theory.

Species[a,b]	$d(OH)_{1,a}$	$d(CO)_{1,a}$	$d(CO)_{1,b}$	$d(OH)_{2,a}$	$d(CO)_{2,a}$	$d(CO)_{2,b}$	$d(C_1\text{-}C_2)$	d(B-B)	d(B-C)	d(B-H)/Å	^{o}COO/H-COO/H
						o-carborane dicarboxylic					
Neutral	0.977	1.331	1.215	0.977	1.329	1.216	3.120	1.78	1.73	1.18	84.3
Monoanion		1.254	1.255	0.977	1.334	1.216	3.180	1.78	1.72	1.18	86.6
Monoanion[c]		1.278	1.238	1.100	1.300	1.230	3.508	1.78	1.72	1.18	0.03
Dianion		1.255	1.257		1.257	1.256	3.214	1.78	1.73	1.18	59.7
						m-carborane dicarboxylic					
Neutral	0.977	1.334	1.218	0.977	1.334	1.218	5.129	1.78	1.72	1.18	0.01
Monoanion		1.258	1.259	0.976	1.336	1.218	5.203	1.78	1.72	1.18	11.4
Dianion		1.260	1.259		1.259	1.260	5.284	1.78	1.71	1.18	47.0
						p-carborane dicarboxylic					
Neutral	0.977	1.336	1.218	0.977	1.336	1.218	6.123	1.78	1.72	1.18	86.6
Monoanion[d]		1.246	1.246	0.972	1.356	1.213	6.240	1.77	1.72	1.18	88.9
Dianion		1.260	1.261		1.261	1.260	6.236	1.77	1.72	1.18	82.8

[a] Atom numbering shown in **Fig. 14**

[b] Distances in Å

[c] Intramolecular H-bonded geometry

[d] Calculation in the gas phase

6.1.3 *Phthalic acids*

Similarly, the geometry of the phthalic acids molecules was optimized at the B3LYP/6-31+G(d,p) level of theory for optimizations in the gas phase and using the SMD/B3LYP/6-31+G(d,p) level of theory for optimizations in water. Then, PES was obtained rotating both carboxyl groups 360° (taking 30° each rotation).

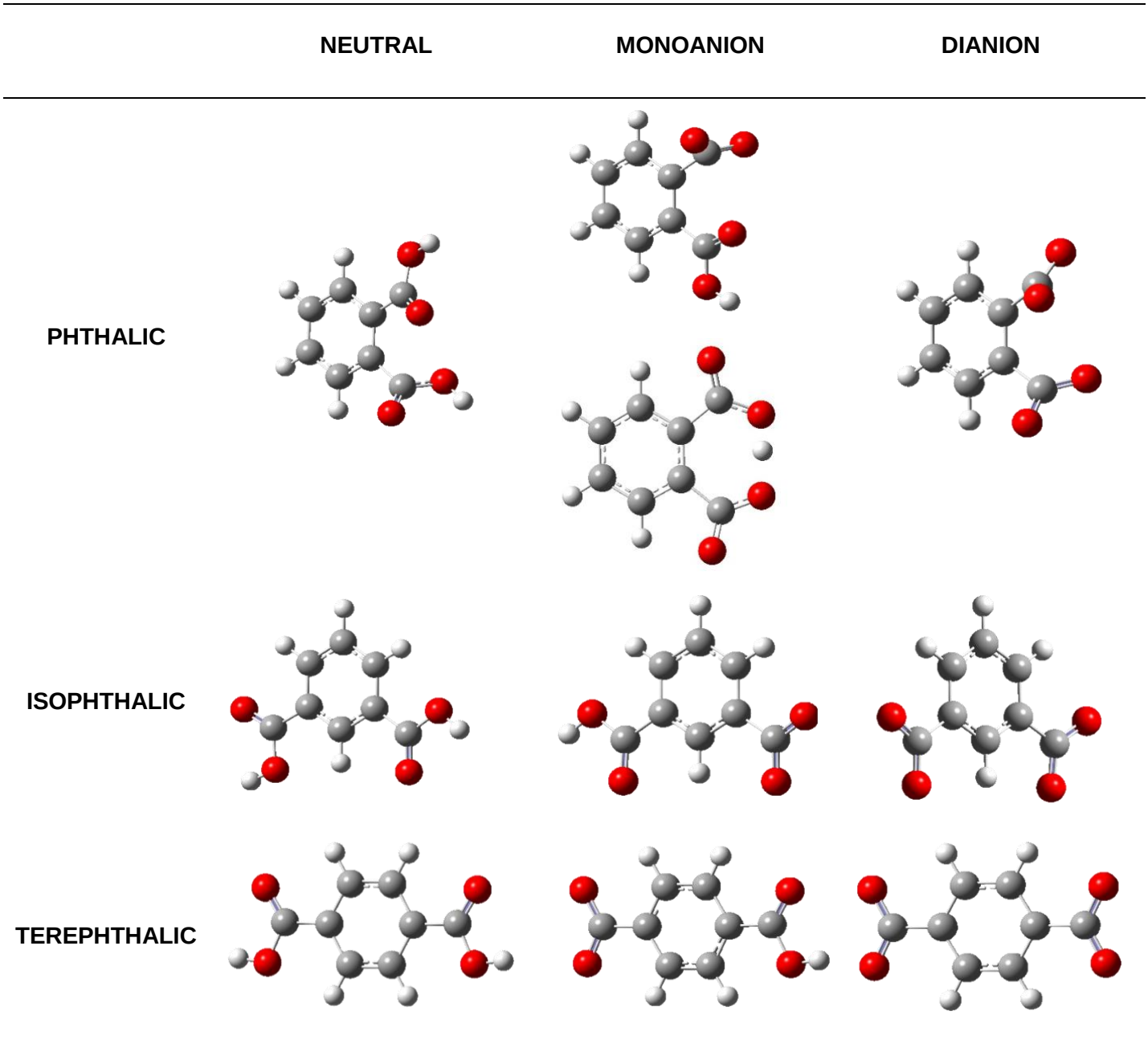

Figure 20. Optimized structures of phthalic acids for the *ortho-, meta-* and *para-* isomers (neutral, monoanion and dianion) in water at the SMD/B3LYP/6-31+G(d,p) level of theory.

Table 6. Geometric parameters of phthalic acids in water. SMD/B3LYP/6-31+G(d,p) level of theory.

Species[a,b]	$d(OH)_{1,a}$	$d(CO)_{1,a}$	$d(CO)_{1,b}$	$d(OH)_{2,a}$	$d(CO)_{2,a}$	$d(CO)_{2,b}$	$d(C_1\text{-}C_2)$	^{o}COO/H-COO/H
					Phthalic			
Neutral	0.976	1.344	1.223	0.975	1.347	1.226	2.988	62.90
Monoanion		1.266	1.266	0.975	1.354	1.227	3.021	78.95
Monoanion[c]		1.291	1.252	1.083	1.316	1.239	3.273	33.88
Dianion		1.270	1.270		1.270	1.270	3.036	57.25
					Isophthalic			
Neutral	0.975	1.348	1.227	0.975	1.348	1.227	4.994	0.01
Monoanion		1.270	1.270	0.975	1.351	1.228	5.011	7.20
Dianion		1.271	1.272		1.272	1.271	5.074	8.16
					Terephthalic			
Neutral	0.975	1.347	1.226	0.975	1.347	1.226	5.772	0.00
Monoanion		1.269	1.269	0.975	1.351	1.228	5.822	0.11
Dianion		1.271	1.271		1.271	1.271	5.875	0.02

[a] Atom numbering shown in **Fig. 14**

[b] Distances in Å

[c] Intramolecular H-bonded geometry

3D potential energy surfaces were obtained, having all of them a shape similar to that of carborane dicarboxylic acids (see **Fig. 18**). As before, the minima of the conformational search were optimized at the B3LYP/6-31+G(d,p) level of theory in the gas phase and using the SMD/B3LYP/6-31+G(d,p) level in water. The most stable structures obtained for the phthalic acids in water are gathered in **Fig. 20** and the optimized geometric parameters are listed in **Table 6.**

The values obtained present the same trend as carborane dicarboxylic acids. The main differences are in the values of the angle in between carboxyl/carboxylate groups. In isophthalic and terephthalic species they are nearly coplanar, whereas for *ortho*-phthalic isomers is not far from 65º. This time carboxyl and carboxylate groups do not lie in the same plane (ca. 30º) due to steric hindrance.

6.1.4 Electronic parameters

6.1.4.1 Atomic Charges and dipole moments

Calculated dipole moments and Mulliken atomic charges for phthalic and carborane dicarboxylic acids are collected in **Tables 7 & 8.** Carborane dicarboxylic and phthalic acids show similar trends as regards to dipole moment and atomic charges. Again, data for the monoanion of p-carborane dicarboxylic acid should be taken with caution the reported values come gas phase calculation.

The dipole moment of the neutral species follows the order: *ortho*- > *para*- > *meta*-, and slightly higher for phthalic than for carborane dicarboxylic. Acidic protons bear more positive charge in the case of carboranes. As expected on chemical grounds, there are less negative charge on oxygens bond to acidic hydrogens than on the other oxygen of the carboxyl group, negative charge that equalizes after deprotonation. The negative charge on the oxygens of neutral, monoanion and dianion species is higher on phthalic acids.

The positive charge of the carbon atom of the carboxyl/carboxylate group increases in going from neutral to charged species for *ortho*-isomer, the opposite happens for *meta*- and *para*-isomers. When carboxyl/carboxylate group is considered as an entity, all neutral species bear positive charge on both carboxyl groups, but just in one o-phthalic acid. After the first deprotonation, the carboxylate group achieves negative charge, whereas the charge on the remaining carboxyl group slightly decreases, but still it is positive. Once the second deprotonation has taking place, the negative charge on both carboxylate groups equalizes.

Table 7. Mulliken atomic charges and dipole moments of carborane dicarboxylic acids in water. SMD/B3LYP/6-31++G(d,p) level of theory.

Species[a,b]	μ / D	$q(H)_{1,a}$	$q(O)_{1.a}$	$q(O)_{1,b}$	$q(C)_1$	$qCO_2^-/H(CO_2^-/H)_a$	$q(H)_{2,a}$	$q(O)_{2,a}$	$q(O)_{2,b}$	$q(C)_2$	$qCO_2^-/H(CO_2^-/H)_b$
					o-carborane dicarboxylic						
Neutral	5.25	0.473	-0.360	-0.375	0.384	0.122	0.462	-0.347	-0.399	0.399	0.115
Monoanion			-0,593	-0.608	0.433	-0.768	0.468	-0.371	-0.393	0.363	0.067
Monoanion[c]			-0,519	-0.543	0.483	-0.579	0.593	-0.566	-0.474	0.440	-0.007
Dianion			-0.619	-0.628	0.476	-0.771		-0.606	-0.617	0.427	-0.796
					m-carborane dicarboxylic						
Neutral	1.00	0.472	-0.386	-0.448	0.607	0.245	0.472	-0.386	-0.448	0.607	0.245
Monoanion			-0.640	-0.644	0.479	-0.805	0.470	-0.389	-0.455	0.568	0.194
Dianion			-0.657	-0.637	0.445	-0.849		-0.637	-0.657	0.445	-0.849
					p-carborane dicarboxylic						
Neutral	3.15	0.471	-0.395	-0.452	0.476	0.100	0.471	-0.399	-0.451	0.499	0.120
Monoanion[d]			-0.487	-0.485	0.172	-0.800	0.392	-0.342	-0.355	0.299	-0.006
Dianion			-0.664	-0.653	0.401	-0.916		-0.654	-0.661	0.400	-0.915

[a] Atom numbering shown in **Fig. 14**

[b] Charges in atomic units

[c] Intramolecular H-bonded geometry

[d] Calculation in the gas phase

Table 8. Mulliken atomic charges and dipole moments of phthalic acids in water. SMD/B3LYP/6-31+G(d,p) level of theory.

Species[a,b]	μ / D	$q(H)_{1,a}$	$q(O)_{1.a}$	$q(O)_{1,b}$	$q(C)_1$	$qCO_2^-/H(CO_2^-/H)_a$	$q(H)_{2,a}$	$q(O)_{2,a}$	$q(O)_{2,b}$	$q(C)_2$	$qCO_2^-/H(CO_2^-/H)_b$
						Phthalic					
Neutral	5.31	0.434	-0.441	-0.517	0.272	-0.252	0.443	-0.496	-0.558	0.835	0.224
Monoanion			-0,672	-0.670	0.420	-0.922	0.443	-0.518	-0.598	0.810	0.137
Monoanion[c]			-0,727	-0.690	0.711	-0.706	0.513	-0.629	-0.646	0.638	-0.124
Dianion			-0.723	-0.736	0.620	-0.839		-0.736	-0.723	0.619	-0.840
						Isophthalic					
Neutral	3.19	0.450	-0.526	-0.594	0.961	0.291	0.448	-0.521	-0.598	0.975	0.304
Monoanion			-0.773	-0.772	0.885	-0.660	0.446	-0.525	-0.607	0.970	0.284
Dianion			-0.780	-0.780	0.868	-0.692		-0.780	-0.780	0.868	-0.692
						Terephthalic					
Neutral	4.52	0.449	-0.520	-0.591	1.062	0.400	0.449	-0.520	-0.591	1.062	0.400
Monoanion			-0.769	-0.769	0.922	-0.616	0.447	-0.525	-0.604	1.062	0.380
Dianion			-0.779	-0.779	0.930	-0.628		-0.779	-0.779	0.930	-0.628

[a] Atom numbering shown in **Fig. 14**

[b] Charges in atomic units

[c] Intramolecular H-bonded geometry

6.1.4.2 Molecular orbitals

It is well known that chemical reactivity is mainly controlled by higher occupied and lower virtual MOs, principally frontier orbitals *i.e.* the highest occupied molecular orbital (HOMO) and the lower occupied molecular orbital (LUMO). Here the discussion of MOs has been restricted from HOMO -1 to LUMO +1 for phthalic and carborane dicarboxylic acids and from HOMO to LUMO for benzoic acid (**Fig. 21)**. Similar patterns were obtained for the rest of compounds. HOMO, LUMO and $E_{LUMO} - E_{HOMO}$ energies for the compounds studied here have been collected in **Table 9**.

Table 9. HOMO & LUMO energy values for the studied compounds

Species[a]	HOMO	LUMO	$E_{LUMO} - E_{HOMO}$
o-carborane dicarboxylic			
Neutral	-8.480	-1.552	6.93
Monoanion	-7.325	-1.303	6.02
Monoanion[b]	-7.699	-1.175	6.52
Dianion	-7.030	-0.467	6.56
m-carborane dicarboxylic			
Neutral	-8.361	-1.641	6.72
Monoanion	-7.074	-1.308	5.77
Dianion	-6.927	-0.520	6.41
p-carborane dicarboxylic			
Neutral	-8.384	-1.348	7.04
Monoanion[c]	-2.517	-1.387	3.90
Dianion	-6.955	-0.350	6.61
Benzoic			
Neutral	-7.258	-1.781	5.48
Monoanion	-6.778	-1.015	5.76
Phthalic			
Neutral	-7.420	-1.997	5.42
Monoanion	-6.568	-1.707	4.86
Monoanion[b]	-7.036	-1.740	5.30
Dianion	-6.305	-0.753	5.55
Isophthalic			
Neutral	-7.553	-2.095	5.46
Monoanion	-6.833	-1.779	5.05
Dianion	-6.690	-1.137	5.55
Terephthalic			
Neutral	-7.489	-2.479	5.01
Monoanion	-6.871	-2.010	4.86
Dianion	-6.727	-1.398	5.33

[a] Energies in eV

[b] Intramolecular H-bonded geometry

[c] Calculation in the gas phase

Species	LUMO +1	LUMO	HOMO	HOMO -1
meta-carborane dicarboxylic Acid	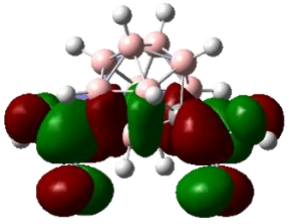	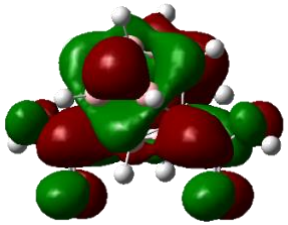	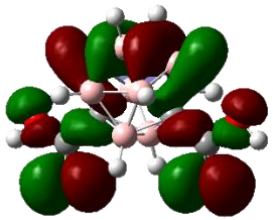	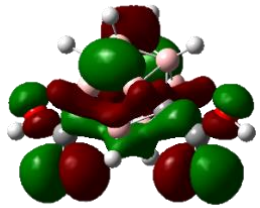
Monoanion *meta*-carborane dicarboxylic Acid	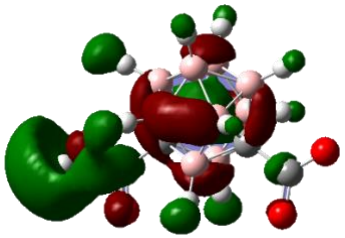	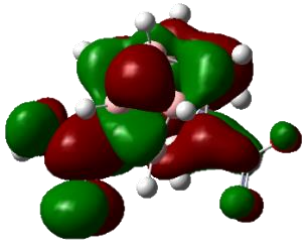	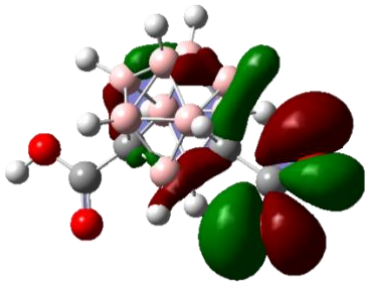	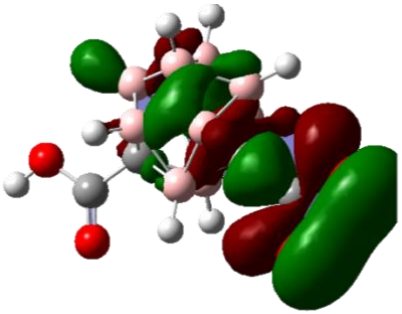
Dianion *meta*-carborane dicarboxylic acid	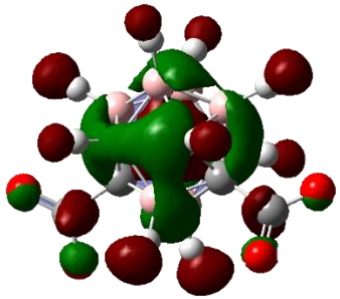	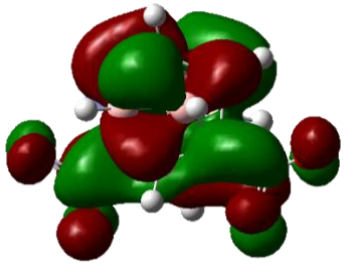	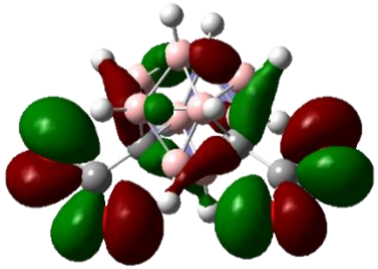	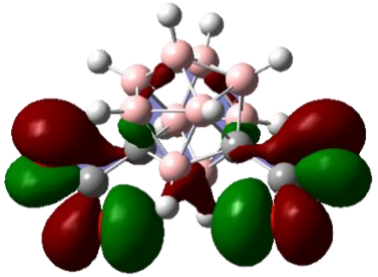

Figure 21. Selected MOs for *meta*-carborane dicarboxylic acid. SMD/B3LYP/6-31++G(d,p) level of theory

For the neutral *meta*-carborane dicarboxylic acid, the charge density of these MOs is localized symmetrically as a consequence of an existing symmetry plane. After the first deprotonation, the charge density rearranges; it mostly localizes on the carboxyl-group containing the second acidic hydrogen, LUMO +1 and LUMO orbitals, and concentrates on the deprotonated carboxyl-group, HOMO and HOMO -1. The pattern observed for the dianion is the same as that of the neutral species, as the initial symmetry recovers after the second deprotonation. The shape of HOMO and HOMO -1 orbitals is similar within each acid. Moreover, some resemblance exists in between the HOMO and HOMO -1 of neutral and dianionic species, and LUMO remains almost unchanged regardless the specie.

6.1.5 IR spectra

Calculation of optimized structures also allows the simulation of IR spectra. In fact, both items are closely related, as an easy way to know if the obtained structure is at least a local minimum on the PES is by checking that all vibrational frequencies are positive, which is equivalent to meet a mathematical minimum. **Table 10** shows the obtained frequencies for the O-H stretching vibration of the studied compounds. Those values, as well as the calculated ones, have been calculated using the rigid rotor and harmonic oscillator approximations.

Table 10. IR wavenumbers for the O-H stretching vibration of the studied acids calculated at the SMD/B3LYP/6-31++G(d,p) level of theory for carborane dicarboxylic and at the SMD/B3LYP/6-31+G(d,p) level of theory for phthalic acids.

Species[a]	**$(OH)_1$ / cm^{-1}**	**$(OH)_2$ / cm^{-1}**	**$(OH)_1$ / cm^{-1}**	**$(OH)_2$ / cm^{-1}**
	Phthalic		Carborane dicarboxylic	
o-Neutral	3718	3698	3701	3698
o-Monoanion		3725		3708
o-Monoanion[b]	1503	1819	1758	1463
m-Neutral	3727	3725	3702	3702
m-Monoanion		3731		3704
p-Neutral[c]	3722	3722	3704	3703
p-Monoanion		3716		3759 [b]

[a] 3729 cm^{-1} obtained for benzoic acid
[b] $O_{1,a}\cdots H_{2,b}–O_{2,b}$ intramolecular H-bond (weak)
[c] Calculation in the gas phase

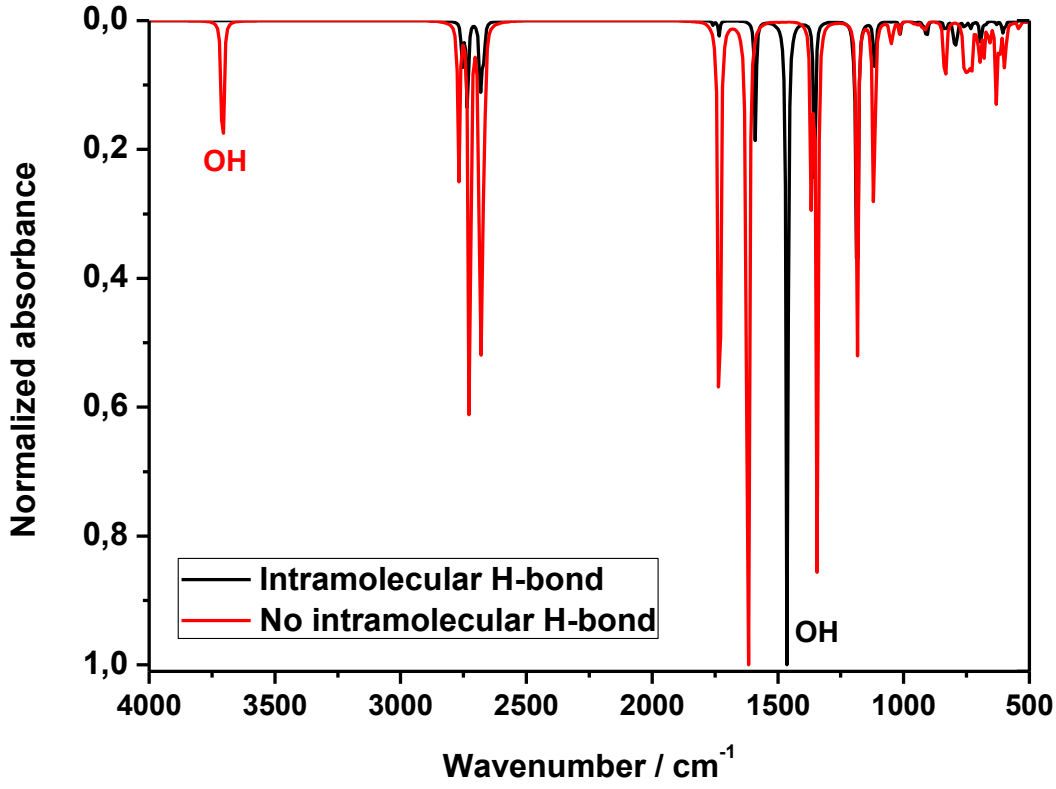

Figure 22. Predicted IR spectra of the monoanion of *ortho*-carborane dicarboxylic acid. Red: No intramolecular hydrogen bond; black: Intramolecular H-bond (**$O_{1,a}\cdots H_{2,b}$--$O_{2,a}$**). Half-width at Half Height: 4 cm^{-1}. SMD/B3LYP/6-31++G(d,p) level of theory

The values collected in **Table 10** are consistent with the experimental ones obtained for this vibration in the case of carboxylic acids in aqueous solution.[xli]

The red line in **Fig. 22** corresponds to a typical IR spectrum of carborane dicarboxylic acids, obviously peaks related to vibrations involving the hydrogen atom of carboxyl groups will be absent for dianions. This figure shows a comparison between the predicted spectrum for the monoanion of *ortho*-carborane dicarboxylic acid with (black line) and without the intramolecular H-bond (**$O_{1,a}\cdots H_{2,b}$--$O_{2,a}$**). In the case of the intramolecular H-bonded species, the OH stretching vibration falls out to lower wavenumber, from *ca.* 3700 cm^{-1} to *ca.* 1500 cm^{-1}. IR spectra of both species were normalized for ease comparison.

6.2 Acidity Constants

Acidity constants for the studied compounds were calculated using the six methods described in chapter 4. Obtained values for benzoic acid and phthalic acids are collected in **Table 11**. The table includes pK_a values calculated using two different basis sets in method 1 to analyze the effect of the basis set. As stated in chapter 4 and following the procedure of Psciuk *et al*, [xlii]single point gas phase calculations using the aug-cc-pVTZ basis set were carried out to get more accurate electronic energies; however, such improvement in electronic energy does not provide better pK_a values, they are worse than those obtained with 6-31++G(d,p) and 6-31+G(d,p) basis set.

Values in **Table 11** suggest that the most suitable method for acidity constants calculation of benzoic and phthalic acids is method 6, *i.e.*, calculation of electronic energy, ZPE and thermal corrections for the process:

$$AH_n^{n-2}(g) + H_2O(g) \underset{\rightarrow}{\leftarrow} AH_{n-1}^{n-3}(g) + H_3O^+(g)$$

together with the calculation of the solvation energy of AH_n^{n-2} and AH_{n-1}^{n-3} (with n 1 or 2) and taking into account the empirical values for H_2O (-26.44 kJ·mol^{-1}) and H_3O^+ (-461.08 kJ·mol^{-1}) solvation energy. Results obtained with method 6 match experimental values within two pK_a units.

The trend observed for phthalic acids is the following:

$$pK_{a,1}phthalic\ bond \ll pK_{a,1}terephthalic < pK_{a,1}isophthalic$$

$$pK_{a,2}phthalic\ bond < pK_{a,2}isophthalic \approx pK_{a,2}terephthalic$$

Although the monoanion of the phthalic acid involving an intramolecular hydrogen bond, $O_{1,a}\cdots H_{2,b}\cdots O_{2,b}$ (see **Fig. 20**), is more stable than in its absence, it seems such specie is not relevant in the corresponding acid-base equilibria. The obtained pKa value, without intramolecular hydrogen bond, is close to the experimental one. Assuming a mean deviation of two pK units relative to the experimental value, the expected experimental pK_a, with intramolecular H-bond, should be *ca.* 0.5, far from the empirical (*ca.* 3).

pK_a calculations for carboranes dicarboxylic acids were performed as well with the six methods. Calculated pK_a values for the carborane dicarboxylic acids under study are listed in **Table 12.**

Table 11. pK_a values obtained for benzoic and phthalic acids using the methods described in chapter 4.

pK_a	$AH \rightarrow A^- + H^+$			$AH + R^- \rightarrow A^- + RH$	$AH + H_2O \rightarrow A^- + H_3O^+$			
	Method 1		Method 2	Method 3	Method 4	Method 5	Method 6	Experimental[xliii]
	6-31+G(d,p)	6-31+G(d,p)// aug-cc-pVTZ		Isodesmic				
					Benzoic			
pK_a	5.62	6.37	6.17		19.46	17.29	**5.23**	4.17
					Phthalic			
$pK_{a.1}$	3.47	4.21	4.02	2.05	17.30	15.14	**3.09**	2.943
$pK_{a.2}$	6.11	7.25	6.59	4.62	19.88	17.78	**5.73**	5.432
					Phthalic intramolecular H-bond			
$pK_{a.1}$	-1.23	-0.01	0.18	-1.79	13.47	10.44	**-1.61**	2.943
$pK_{a.2}$	10.81	11.47	10.42	8.45	23.71	22.48	**10.43**	5.432
					Isophthalic			
$pK_{a.1}$	4.44	5.24	5.08	3.11	18.36	16.11	**4.06**	3.70
$pK_{a.2}$	6.59	8.13	6.77	4.80	20.05	18.31	**6.26**	4.60
					Terephthalic			
$pK_{a.1}$	4.14	4.93	4.70	2.73	17.99	15.81	**3.76**	3.54
$pK_{a.2}$	6.59	8.14	6.47	4.50	19.76	18.26	**6.21**	4.34

Table 12. pK_a values obtained for carborane dicarboxylic acids using the methods described in chapter 4.

pK_a	$AH \rightarrow A^- + H^+$			$AH + R^- \rightarrow A^- + RH$	$AH + H_2O \rightarrow A^- + H_3O^+$		
	Method 1		Method 2	Method 3	Method 4	Method 5	Method 6
	6-31++G(d,p)	6-31++G(d,p)// aug-cc-pVTZ		Isodesmic			
				o-carborane dicarboxylic			
$pK_{a.1}$	-1.12	-0.38	-1.25	-3.22	12.03	-1.50	10.55
$pK_{a.2}$	1.42	2.39	2.56	0.59	15.85	1.04	13.09
				o-carborane dicarboxylic (intramolecular H-bond)			
$pK_{a.1}$	-5.78	-4.89	-4.82	-6.79	8.46	-6.16	5.89
$pK_{a.2}$	6.08	6.90	6.13	4.16	19.42	5.70	17.75
				m-carborane dicarboxylic			
$pK_{a.1}$	0.80	1.49	1.04	-0.93	14.33	0.42	12.47
$pK_{a.2}$	2.50	3.68	2.58	0.61	15.87	2.11	14.17
				p-carborane dicarboxylic			
$pK_{a.1}$	2.32	2.97	-	-	-	1.94	13.99
$pK_{a.2}$	1.16	2.28	-	-	-	0.78	12.83

The major difference in pK_a values ($pK_{a,1}$ & $pK_{a,2}$) is observed for *ortho*-carborane dicarboxylic acid when compared to *meta* and *para*. *Ortho* isomer is observed to be the most acidic, *i.e.*, lowest pK_{a1}. The trend, should be similar to that of phthalic acids, is the following:

$$pK_{a,1}ortho \ll pK_{a,1}meta < pK_{a,1}para$$

$$pK_{a,2}ortho < pK_{a,2}para < pK_{a,2}meta$$

Those pK_{a2} values should be considered with caution since the quantum-chemical computation of solvated doubly charged anions is less reliable as compared to monovalent anions.

Calculations involving the *p*-carborane dicarboxylate did not run properly for unknown reasons, similar facts have been reported with this species. [xliv] From there it follows that obtained results, in gray, should be considered with caution.

In a broad send, carborane dicarboxylic acids can be considered as phthalic acids where the carborane cage replaced the benzene ring. Carborane dicarboxylic acids present higher acidity than their parent phthalic acids, *ca.* four pK_a units both in $pK_{a,1}$ and $pK_{a,2}$. On the other hand, similar differences between $pK_{a,1}$ and $pK_{a,2}$ are found in phthalic and carborane dicarboxylic acids for a given compound.

Again, much higher acidity is calculated for the first dissociation constant of *ortho* carborane dicarboxylic acid. It is expected to be a consequence of the formation of the $O_{1,a}\cdots H_{2,b}\cdots O_{2,b}$ bridge (**Fig. 19).** Similarly to *o*-phthalic acid, the intramolecular hydrogen bonded structure will not have relevance in the corresponding acid-base equilibria, therefore $pK_{a,1}$ and $pK_{a,2}$ for *o*-carborane dicarboxylic acid should be close to -1.5 and 1.0, respectively.

Acidity constants were calculated using the most stable species, i.e. those found after geometry optimization, this means it has been assumed no other conformations contribute to the pK_a. Such assumption can be accepted as other conformations show slightly higher energies, less than 4 $kJ{\cdot}mol^{-1}$ (**Table 4**). Those differences in energy cause small error in pK_a calculation compared to errors associated to solvation energies, mainly in the case of doubly charged species. Therefore, the obtained pK_a values with method 6 should fit the experimental ones within two pK units.

6.3 Determination of Redox Potentials

One-electron reduction potential calculations were carried out for benzoic and some carborane dicarboxylic acids and their corresponding monoanion and dianion, they are collected in **Table 13.** As stated in chapter 4, absolute one-electron reduction potentials were calculated, but for comparison purposes, they have been reported as values relative to SHE.

Table 13. E° values (V) –relative to SHE– obtained for benzoic acid and carborane dicarboxylic acids using the methods described in chapter 4.

Process	Method 1		Method 2
	6-31++G(d,p)	6-31++G(d,p)// aug-cc-pVTZ	
	Benzoic		
$AH + e^- \rightarrow AH^{\cdot -}$	-1.84	-5.45	-1.87
$A^{\cdot} + e^- \rightarrow A^{\cdot -}$	1.80	5.37	1.78
$A^- + e^- \rightarrow A^{\cdot 2-}$	-2.72	-6.29	-2.61
	m-carborane dicarboxylic		
$AH_2^{\cdot +} + e^- \rightarrow AH_2$	3.53	3.53	3.56
$AH_2 + e^- \rightarrow AH_2^{\cdot -}$	-1.95	-1.97	-1.85
$AH^{\cdot} + e^- \rightarrow AH^-$	2.17	2.18	2.18
$A^{\cdot -} + e^- \rightarrow A^{2-}$	2.07	2.08	2.04
	p-carborane dicarboxylic		
$A^{\cdot -} + e^- \rightarrow A^{2-}$	1.96	1.92	2.02

As UHF calculations handle with open shell species, geometry optimizations usually experience convergence problems; this explains the limited number of reduction potentials reported here.

Obtained values seem independent of the method and of the basis set, the only exception are the potentials of benzoic acid and benzoate anion calculated at the 6-31++G(d,p)//aug-cc-pVTZ level of theory, which are nonsense. Reduction potentials of closed shell neutral species are negative, whereas positive reduction potentials were calculated for the one-electron reduction of radical species.

Those negative values are similar to those reported for esters and carboxylic acids. On the other hand, positive values are slightly higher than carboxylates.[xlv]

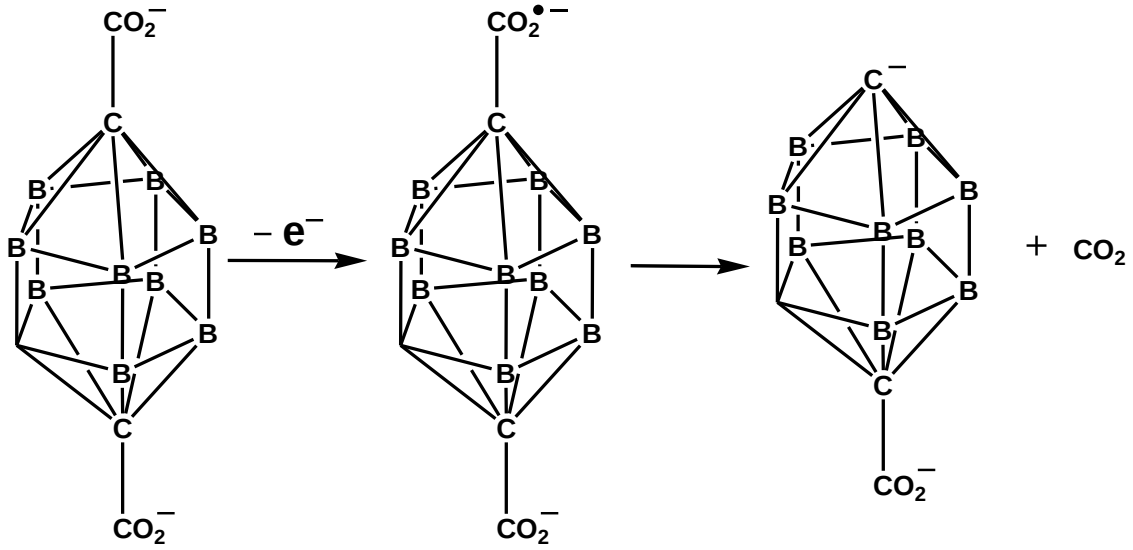

Figure 23. Decarboxylation of the one-electron oxidation of the dianion of para-carborane dicarboxylic acid

The case of the one-electron reduction to give the dianion of the *para*-carborane dicarboxylic acid merits especial mention as likely the corresponding radical anion decarboxylates, as shown in the previous figure. Loss of CO_2 is a common process when this type of radicals is formed. A second decarboxylation could be taken place due to the instability of the so-formed dianion, and likely the charged carborane also breaks.

7. CONCLUSIONS

Electronic structure calculations on 1,2-closo-dicarbadodecaborane-1,2-dicarboxylic acid, 1,7-closo-dicarbadodecaborane-1,7-dicarboxylic acid, 1,12-closodicarbadodecaborane-1,12-dicarboxylic acid, benzoic acid, phthalic, isophthalic and terephthalic acids and that of their corresponding anions after the first and the second deprotonation, using the Density Functional Theory (DFT) with 6-31++G(d,p) as basis set, and the solvation model based on density (SMD) to simulate water as a solvent, lead to the following conclusions:

1. Corresponding geometrical parameters for carborane dicarboxylic acids and phthalic acids, and for their anions, for the optimized structures after the conformational study are similar and within the expected values for this kind of compounds.
2. Selected electronic parameters also evidenced to be similar for carborane dicarboxylic and phthalic acids, and their anions. *Ortho*-isomers present differences due to the formation of an intramolecular hydrogen bond, which stabilizes the carboxylate group.
3. Simulated IR spectra, using the rigid rotor and harmonic oscillator approximation, resemble experimental ones. Frequency of the OH stretching vibration matches the value measured for carboxylic acids in aqueous solution.
4. Calculation of the acidity constants was compared using six methods. Values closer to empirical ones, within two pK units, were found using a thermodynamic cycle and the empiric values for the solvation energy of H_2O and H_3O^+. The use of a more sophisticated basis set does not improve the results.
5. Higher acidity was found for carborane dicarboxylic acids than for phthalic acids in both deprotonation equilibria. O*rtho*-isomer is more acid when compared to the other positional isomers.
6. One-electron reduction potentials were calculated using two methods; similar results were obtained. Calculated values fit well that of reported in the literature for carboxylic acids and carboxylates.
7. The calculation involving the one-electron oxidized form of the dianion *para*-carborane dicarboxylic acid point to its decarboxylation to release, at least, one CO_2 molecule.

CONCLUSIÓNS

Os cálculos de estrutura electrónica do ácido 1,2-closo-dicarbadodecaborano-1,2-dicarboxílico, ácido 1,7-closo-dicarbadodecaborano-1,7-dicarboxílico, ácido 1,12-closodicarbadodecaborano-1,12-dicarboxílico, ácido benzoico, ácido ftálico, ácido isoftálico e tereftálico e os dos seus anións correspondentes despois da primeira e segunda desprotonación, utilizando a teoría funcional da densidade (DFT) co 6-31++G(d,p) como función base, e o modelo de solvatación baseado na densidade (SMD) para simular auga como disolvente, conducen ás seguintes conclusións:

1. Os parámetros xeométricos correspondentes para ácidos dicarboxílicos de carborano e ácidos ftálicos, e para os seus anións, para as estruturas optimizadas despois do estudo conformacional son similares e están dentro dos valores esperados para este tipo de compostos.
2. Os parámetros electrónicos seleccionados tamén evidenciaron ser similares para os ácidos carboranos dicarboxílicos e ftálicos, e os seus anións. Os *orto*-isómeros presentan diferenzas debido á formación dun enlace de hidróxeno intramolecular, que estabiliza o grupo carboxilato.
3. Os espectros infravermellos simulados, que usan o rotor ríxido e a aproximación do oscilador harmónico, se parecen aos experimentais. A frecuencia da vibración de estiramento OH coincide co valor medido para os ácidos carboxílicos en disolución acuosa.
4. O cálculo das constantes de acidez comparouse utilizando seis métodos. Os valores máis pretos aos empíricos, dentro de dúas unidades de pK, se atoparon utilizando un ciclo termodinámico e os valores empíricos para a enerxía de solvatación de H_2O e H_3O^+. O uso dunha función base máis sofisticada non mellora os resultados.
5. Atopouse unha acidez máis alta para os ácidos dicarboxílicos de carborano que para os ácidos ftálicos en ambos equilibrios de desprotonación. O *orto*-isómero é más ácido en comparación cos outros isómeros posicionais.
6. Os potenciais de redución monoelectrónicos se calcularon usando dous métodos; resultados similares foron obtidos. Os valores calculados se axustan ben aos descritos na bibliografía para ácidos carboxílicos e carboxilatos.
7. O cálculo que implica a forma oxidada dun electrón do ácido dianiónico *para*-carborano dicarboxílico apunta á súa descarboxilación para liberar, ao menos, unha molécula de CO2.

CONCLUSIONES

Los cálculos de estructura electrónica del ácido 1,2-closo-dicarbadodecaborano-1,2-dicarboxílico, ácido 1,7-closo-dicarbadodecaborano-1,7-dicarboxílico, ácido 1,12-closodicarbadodecaborano-1,12-dicarboxílico, ácido benzoico, ácido ftálico, ácido isoftálico y tereftálico y los de sus aniones correspondientes después de la primera y la segunda desprotonación, utilizando la teoría de función
al de la densidad (DFT) con 6-31++G(d,p) como función base, y el modelo de solvatación basado en la densidad (SMD) para simular agua como disolvente, conducen a las siguientes conclusiones:

1. Los parámetros geométricos correspondientes para ácidos dicarboxílicos de carborano y ácidos ftálicos, y para sus aniones, para las estructuras optimizadas después del estudio conformacional son similares y están dentro de los valores esperados para este tipo de compuestos.
2. Los parámetros electrónicos seleccionados también evidenciaron ser similares para los ácidos carboranos dicarboxílicos y ftálicos, y sus aniones. Los *orto*-isómeros presentan diferencias debido a la formación de un enlace de hidrógeno intramolecular, que estabiliza el grupo carboxilato.
3. Los espectros infrarrojos simulados, que usan el rotor rígido y la aproximación del oscilador armónico, se parecen a los experimentales. La frecuencia de la vibración de estiramiento OH coincide con el valor medido para los ácidos carboxílicos en disolución acuosa.
4. El cálculo de las constantes de acidez se comparó utilizando seis métodos. Los valores más cercanos a los empíricos, dentro de dos unidades de pK, se encontraron utilizando un ciclo termodinámico y los valores empíricos para la energía de solvatación de H_2O y H_3O^+. El uso de una función base más sofisticada no mejora los resultados.
5. Se encontró una acidez más alta para los ácidos dicarboxílicos de carborano que para los ácidos ftálicos en ambos equilibrios de desprotonación. El *orto*-isómero es más ácido en comparación con los otros isómeros posicionales.
6. Los potenciales de reducción monoelectrónicos se calcularon usando dos métodos; resultados similares fueron obtenidos. Los valores calculados se ajustan bien a los descritos en la bibliografía para ácidos carboxílicos y carboxilatos.

7. El cálculo que implica la forma oxidada de un electrón del ácido dianiónico *para*-carborano dicarboxílico apunta a su descarboxilación para liberar, al menos, una molécula de CO_2.

8. BIBLIOGRAPHY

[i] Grimes, R. N. Chapter 1 - Introduction and History. In *Carboranes (Second Edition)*; Grimes, R. N., Ed.; Academic Press: Oxford, 2011; pp 1-6.

[ii] *http://epgp.inflibnet.ac.in/epgpdata/uploads/epgp_content/chemistry/inorganic_chemistry-iii/23.structure_and_bonding_of_carboranes/et/4838_et_et.pdf* Last access 17/06/2018.

[iii] Valliant, J. F.; Guenther, K. J.; King, A. S.; Morel, P.; Schaffer, P.; Sogbein, O. O.; Stephenson, K. A. The medicinal chemistry of carboranes. *Coordination Chemistry Reviews* **2002***, 232*, 173-230.

[iv] Issa, F.; Kassiou, M.; Rendina, L. Boron in Drug Discovery: Carboranes as Unique Pharmacophores in Biologically Active Compounds. *Chem. Rev.* **2011***, 111*, 5701-5722.

[v] Grimes, R. N. Chapter 2 - Structure and Bonding. In *Carboranes (Second Edition)*; Grimes, R. N., Ed.; Academic Press: Oxford, 2011; pp 7-20.

[vi] *https://lcbc.epfl.ch/files/content/users/232236/files/Script_IESM_2015-1.pdf* Last access 17/06/2018

[vii] *https://www.lakeheadu.ca/sites/default/files/uploads/31/CHEM_3451_lab_manual_F2013_Comp-Chem.pdf* Last access 17/06/2018

[viii] *http://www.uwyo.edu/kubelka-chem/mm_notes_1.pdf* Last access 17/06/2018

[ix] *https://www.st-andrews.ac.uk/media/school-of-chemistry/documents/Gaussian.pdf* Last access 17/06/2018

[x] Bacharach, S.M. Chapter 1 – Quantum Mechanics for Organic Chemistry. In *Computational Organic Chemistry (First Edition)*; Wiley-Interscience, John Wiley & Sons, Inc. New Jersey (2007). ISBN: 978-0-471-71342-5. pp 1-41

[xi] *https://matin.gatech.edu/groups/materials_informatics_course_fall_2016/wiki/MainPage?version=81* Last access 17/06/2018

[xii] *http://pollux.chem.umn.edu/8021/Lectures/AI_HF_6.pdf* Last access 17/06/2018

[xiii] *http://www.hpc.lsu.edu/training/weekly-materials/2011%20Fall/ElecStruc-2011-11-16.pdf* Last access 17/06/2018

[xiv] *http://rsc.anu.edu.au/~agilbert/gilbertspace/uploads/Chem3108.pdf* Last access 17/06/2018

[xv] *http://www.uwyo.edu/kubelka-chem/mm_notes_9.pdf* Last access 17/06/2018

[xvi] *http://web.uni-plovdiv.bg/vdelchev/physchem/basis%20sets.ppt* Last access 17/06/2018

[xvii] *http://www.helsinki.fi/kemia/fysikaalinen/opetus/jlk/luennot/Lecture5.pdf* Last access 17/06/2018

[xviii] *https://www.southampton.ac.uk/assets/centresresearch/documents/compchem/DFT_L8.pdf* Last access 17/06/2018

[xix] *http://www.helsinki.fi/kemia/fysikaalinen/opetus/Laskennallinen%20kemia/Luennot/Computational%20Chemistry%202016.pdf* Last access 17/06/2018

[xx] *http://web.uvic.ca/~simmater/Groupweb/Qmodule/DFT.pdf* Last access 17/06/2018

[xxi] *https://www.researchgate.net/file.PostFileLoader.html?id=56c32f865e9d97e8268b4588&assetKey=AS%3A329759759323136%401455632261205* Last access 17/06/2018

[xxii] *http://science.sciencemag.org/content/355/6320/49.full* Last access 17/06/2018. DOI: 10.1126/science.aah5975

[xxiii] *http://spindynamics.org/Quantum-Chemistry---Lecture-6.php* Last access 17/06/2018
[xxiv] *http://goldbook.iupac.org/pdf/goldbook.pdf* Last access 17/06/2018
[xxv] *https://events.prace-ri.eu/event/455/material/slides/18.pdf* Last access 17/06/2018
[xxvi] *http://www.crc.nd.edu/~wschnei1/courses/CBE_547/Lectures/implicit_solvation_models.pdf* Last access 17/06/2018
[xxvii] *http://spindynamics.org/documents/cqc_lecture_8.pdf* Last access 17/06/2018
[xxviii] *https://zdoc.site/quantum-mechanical-continuum-solvation-models-einstennet.html* Last access 17/06/2018
[xxix] *https://www.ncbi.nlm.nih.gov/pubmed/19366259* Last access 17/06/2018. DOI: 10.1021/jp810292n
[xxx] *https://www.cesga.es/es/infraestructuras/computacion/FinisTerrae2* Last access 18/06/2018
[xxxi] *https://www.originlab.com/index.aspx?go.../Origin* Las access 20/06/2018
[xxxii] *http://gaussian.com/* Last access 20/06/2018
[xxxiii] *http://www.perkinelmer.com/ChemDraw* Last access 20/06/2018
[xxxiv] *http://mercuryconsortium.org/furman/pubs/AlongiS2010.pdf* Last access 17/06/2018. DOI: 10.1016/S1574-1400(10)06008-1
[xxxv] Psciuk, B. T.; Lord, R. L.; Munk, B. H.; Schlegel, H. B. Theoretical Determination of One-Electron Oxidation Potentials for Nucleic Acid Bases. *J. Chem. Theory Comput.* **2012***, 8*, 5107-5123.
[xxxvi] Oliva-Enrich, J. M.; Humbel, S.; Santaballa, J. A.; Alkorta, I.; Notario, R.; Davalos, J. Z.; Canle-L, M.; Bernhardt, E.; Holub, J.; Hnyk, D. Predicted Gas-Phase and Liquid-Phase Acidities of Carborane Carboxylic and Dicarboxylic Acids. *ChemistrySelect* **2018***, 3*, 4344-4353.
[xxxvii] Casasnovas, R.; Ortega-Castro, J.; Frau, J.; Donoso, J.; Munoz, F. Theoretical pK(a) Calculations With Continuum Model Solvents, Alternative Protocols to Thermodynamic Cycles. *Int. J. Quantum Chem.* **2014***, 114*, 1350-1363.
[xxxviii] Rossini, E.; Knapp, E. Proton solvation in protic and aprotic solvents. *J. Comput. Chem.* **2016***, 37*, 1082-1091.
[xxxix] *http://support.cas.org/content/chemical-substances/faqs* Last access 20/06/2018
[xl] *https://echa.europa.eu/es/information-on-chemicals/ec-inventory* Last access 20/06/2018
[xli] Max, J.; Chapados, C. Infrared Spectroscopy of Aqueous Carboxylic Acids: Comparison between Different Acids and Their Salts. *J Phys Chem A* **2004***, 108*, 3324-3337.
[xlii] Psciuk, B. T.; Lord, R. L.; Munk, B. H.; Schlegel, H. B. Theoretical Determination of One-Electron Oxidation Potentials for Nucleic Acid Bases. *J. Chem. Theory Comput.* **2012***, 8*, 5107-5123.
[xliii] Kieffer, W. F. CRC Handbook of Chemistry and Physics. 54th Edition. *J. Chem. Educ.* **1975***, 52*, A142.
[xliv] Oliva-Enrich, J. M.; Humbel, S.; Santaballa, J. A.; Alkorta, I.; Notario, R.; Davalos, J. Z.; Canle-L, M.; Bernhardt, E.; Holub, J.; Hnyk, D. Predicted Gas-Phase and Liquid-Phase Acidities of Carborane Carboxylic and Dicarboxylic Acids. *ChemistrySelect* **2018***, 3*, 4344-4353.
[xlv] Roth, H. G.; Romero, N. A.; Nicewicz, D. A. Experimental and Calculated Electrochemical Potentials of Common Organic Molecules for Applications to Single-Electron Redox Chemistry. *Synlett* **2016***, 27*, 714-723.

9. ***ANNEXES***

Annex 1. Gaussian input and output (geometry optimization)

Annex 1a. Typical Gaussian input file

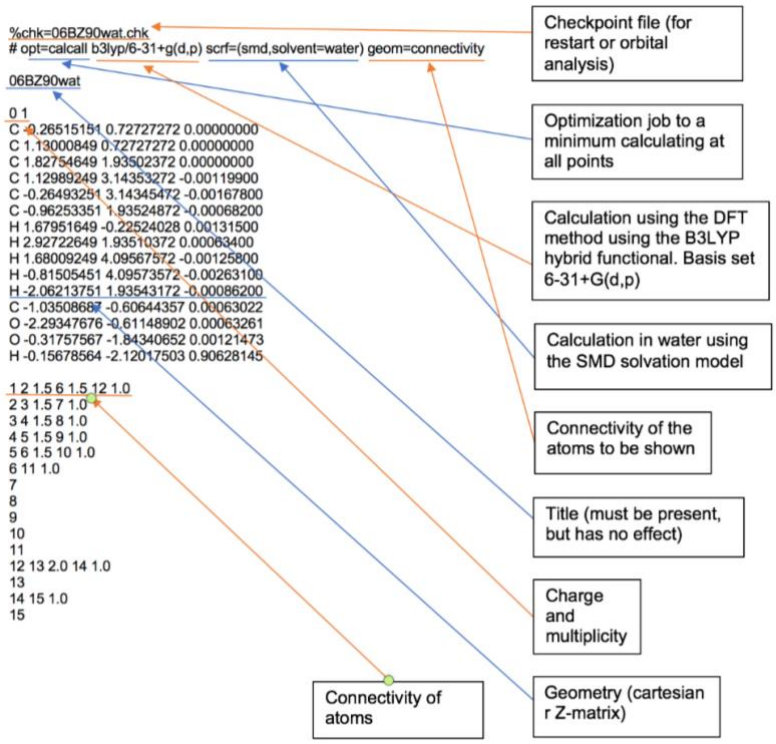

Annex 1b. Selected parts of the Gaussian output

Summary of calculations results:

06BZ90wat		
//Mac/Home/Desktop/TFG/Ficheros/HOME/pKa Ficher...		
File Type	.log	
Calculation Type	FREQ	
Calculation Method	RB3LYP	
Basis Set	6-31+G(d,p)	
Charge	0	
Spin	Singlet	
Solvation	scrf=(smd,solvent=water)	
E(RB3LYP)	-420.861666	Hartree
RMS Gradient Norm	0.000020	Hartree/Bohr
Imaginary Freq	0	
Dipole Moment	7.425675	Debye
Polarizability (α)	127.482667	a.u.
Point Group	C1	
Job cpu time:	**0 days 1 hours 34 minutes 27.0 secon...**	

Standard orientation:

Center Number	Atomic Number	Atomic Type	Coordinates (Angstroms) X	Y	Z
1	6	0	-0.194773	0.052965	-0.015350
2	6	0	0.441552	-1.188560	-0.028616
3	6	0	1.834429	-1.258670	-0.014469
4	6	0	2.591654	-0.086860	0.011757

HOMO & LUMO energy values:

Alpha occ. eigenvalues --	-0.37988	-0.36590	-0.35478	-0.33818	-0.30464
Alpha occ. eigenvalues --	-0.27127	**-0.26806**			
Alpha virt. eigenvalues --	**-0.06402**	-0.02402	0.00555	0.02609	0.02876
Alpha virt. eigenvalues --	0.03294	0.04623	0.05144	0.05327	0.06081

Convergence achievement:

Item		Value	Threshold	Converged?
Maximum	Force	0.000008	0.000450	YES
RMS	Force	0.000003	0.000300	YES
Maximum	Displacement	0.001196	0.001800	YES
RMS	Displacement	0.000225	0.001200	YES

Predicted change in Energy=-5.534544D-09
Optimization completed.
-- Stationary point found.

! Optimized Parameters !
! (Angstroms and Degrees) !

! Name	Definition	Value	Derivative Info.
! R1	R(1,2)	1.4057	-DE/DX = 0.0 !
! R2	R(1,6)	1.4055	-DE/DX = 0.0 !
! R3	R(1,12)	1.4891	-DE/DX = 0.0 !
! R4	R(2,3)	1.3957	-DE/DX = 0.0 !
! R5	R(2,7)	1.0861	-DE/DX = 0.0 !
! R6	R(3,4)	1.3983	-DE/DX = 0.0 !
! R7	R(3,8)	1.0855	-DE/DX = 0.0 !
! R8	R(4,5)	1.3994	-DE/DX = 0.0 !
! R9	R(4,9)	1.0859	-DE/DX = 0.0 !
! R10	R(5,6)	1.3939	-DE/DX = 0.0 !

Mulliken charges:

Mulliken charges:

		1
1	C	0.314682
2	C	-0.199412
3	C	-0.207982
4	C	-0.136531
5	C	-0.208959
6	C	-0.162203
7	H	0.179676
8	H	0.171787
9	H	0.172183
10	H	0.172892

Harmonic frequencies

Harmonic frequencies (cm**-1), IR intensities (KM/Mole), Raman scattering activities (A**4/AMU), depolarization ratios for plane and unpolarized incident light, reduced masses (AMU), force constants (mDyne/A), and normal coordinates:

	1			2			3		
	A			A			A		
Frequencies --	98.8044			163.1187			235.6135		
Red. masses --	6.0450			5.1237			5.7888		
Frc consts --	0.0348			0.0803			0.1893		
IR Inten --	9.9540			4.9202			20.4800		
Atom AN	X	Y	Z	X	Y	Z	X	Y	Z
1 6	0.00	0.02	-0.04	0.00	0.02	0.29	0.00	0.23	-0.07
2 6	-0.02	0.03	0.13	0.01	0.02	0.25	-0.12	0.16	-0.04
3 6	-0.02	0.02	0.19	0.00	-0.02	-0.04	-0.14	-0.05	-0.03
4 6	0.00	-0.01	0.03	0.00	-0.04	-0.27	0.01	-0.14	0.01
5 6	0.01	-0.02	-0.18	0.00	-0.02	-0.07	0.16	-0.05	0.03

System energies

Zero-point correction=	0.115414 (Hartree/Particle)
Thermal correction to Energy=	0.122447
Thermal correction to Enthalpy=	0.123391
Thermal correction to Gibbs Free Energy=	0.083707
Sum of electronic and zero-point Energies=	-420.746252
Sum of electronic and thermal Energies=	-420.739219
Sum of electronic and thermal Enthalpies=	-420.738275
Sum of electronic and thermal Free Energies=	-420.777960

Final comment:

THE RARE EARTHS PERPLEX US IN OUR RESEARCHES,
BAFFLE US IN OUR SPECULATIONS, AND HAUNT US IN OUR
VERY DREAMS. THEY STRETCH LIKE AN UNKNOWN BEFORE US,
MOCKING, MYSTIFYING, AND MURMURING STRANGE REVELATIONS
AND POSSIBILITIES. -- SIR WILLIAM CROOKE, 1832-1919
Job cpu time: 0 days 0 hours 40 minutes 33.3 seconds.
File lengths (MBytes): RWF= 98 Int= 0 D2E= 0 Chk= 11 Scr= 1
Normal termination of Gaussian 09 at Fri Feb 16 13:12:13 2018.

Annex 2. Atomic units and conversion factors[xlv]

Conversion Factors from Atomic to SI units

Atomic unit (base units)	SI values	Name (symbol)
Mass ($m_{e)}$	$9.10939 \cdot 10^{-31}$ kg	Mass of the electron
Charge (e)	$1.602188 \cdot 10^{-39}$ C	Electronic charge
Angular momentum ($\hbar$)	$1.05457 \cdot 10^{-34}$ J/(s rad)	Planck's constant/2π
Energy ($m_e e^4/ \hbar^2$)	$4.35975 \cdot 10^{-18}$ J	Hartree (H)
Length ($\hbar^2/m_e e^2$)	$5.29177 \cdot 10^{-11}$ m	Bohr; Bohr radius (a_0)
Time ($\hbar^3/m_e e^4$)	$2.41888 \cdot 10^{-17}$ s	Jiffy
Electric dipole moment (($\hbar^2/m_e$ e)	$8.47836 \cdot 10^{-30}$ C·m	2.541765 Debye (D) units
Magnetic dipole moment ($e\hbar/2m_e$)	$9.27402 \cdot 10^{-24}$	Bohr magneton (μ_B)

Energy Conversion Table for Non-SI Units

	Value in non-SI units					
Units	a.u.	kcal/mol	eV	cm^{-1}	Hz	K
a.u.	1	$6.27510 \cdot 10^{2}$	$2.72114 \cdot 10^{1}$	$2.19475 \cdot 10^{5}$	$6.57968 \cdot 10^{15}$	$3.15773 \cdot 10^{5}$
kcal/mol	$1.59360 \cdot 10^{-3}$	1	$4.33641 \cdot 10^{-2}$	$3.49755 \cdot 10^{2}$	$1.04854 \cdot 10^{13}$	$5.03217 \cdot 10^{2}$
eV	$3.67493 \cdot 10^{-2}$	$2.30605 \cdot 10^{1}$	1	$8.06554 \cdot 10^{3}$	$2.41799 \cdot 10^{14}$	$1.16044 \cdot 10^{4}$
cm^{-1}	$4.55634 \cdot 10^{-6}$	$2.85914 \cdot 10^{-3}$	$1.23984 \cdot 10^{-4}$	1	$2.99792 \cdot 10^{10}$	1.43877
Hz	$1.51983 \cdot 10^{-16}$	$9.5371 \cdot 10^{-14}$	$4.13567 \cdot 10^{-15}$	$3.33564 \cdot 10^{-11}$	1	$4.79922 \cdot 10^{-11}$
K	$3.16683 \cdot 10^{-6}$	$1.98722 \cdot 10^{-3}$	$8.61739 \cdot 10^{-5}$	$6.95039 \cdot 10^{-1}$	$2.08367 \cdot 10^{10}$	1

Fundamental Constants, in Atomic and SI Units

Physical constant	Symbol	Value (a.u.)	Value (SI)
Rydberg constant	R_∞	$2.29253 \cdot 10^{2}$	$1.09737 \cdot 10^{-23}$/ m
Planck constant	h	6.28319 (2π)	$6.62608 \cdot 10^{-34}$ J·s
Speed of light	c	$1.37036 \cdot 10^{2}$	$2.99792 \cdot 10^{8}$ m/s
Proton mass	m_p	$1.83615 \cdot 10^{3}$	$1.67262 \cdot 10^{-27}$ kg
Atomic Mass unit	amu	$1.82289 \cdot 10^{3}$	$1.66054 \cdot 19^{-27}$ kg
Fine structure constant	α	$7.29735 \cdot 10^{-3}$	$7.29735 \cdot 10^{-3}$

Other Constants and Conversion Factors

Quantity (symbol)	SI value or equivalent
Avogadro's number (N_o)	$6.02214 \cdot 10^{23}$ /mol
Kilocalorie (kcal)	$4.18400 \cdot 10^{3}$ J
Kelvin (K)	C-273.15
Boltzmann constant (k)	$1.38066 \cdot 10^{-23}$ J/K
Faraday constant (F)	$9.65853 \cdot 10^{4}$ C/mol

Annex 3. Statistical correction for pK_a determination in acids with identical protonation/deprotonation sites.

DIPROTIC ACIDS	
First dissociation	
$H_1H_2A \leftrightarrow (H_2A^- + H_1A^-) + H^+$	$K_{a,1} = \frac{([H_2A^-] + [H_1A^-]) \cdot [H^+]}{[H_1H_2A]}$
$H_1H_2A \leftrightarrow H_2A^- + H^+$	$K_{a,1,1} = \frac{[H_2A^-] \cdot [H^+]}{[H_1H_2A]}$ $[H_2A^-] = \frac{K_{a,1,1} \cdot [H_1H_2A]}{[H^+]}$
$H_1H_2A \leftrightarrow H_1A^- + H^+$	$K_{a,1,2} = \frac{[H_1A^-] \cdot [H^+]}{[H_1H_2A]}$ $[H_1A^-] = \frac{K_{a,1,2} \cdot [H_1H_2A]}{[H^+]}$
$K_{a,1} = \frac{\left(\frac{K_{a,1,1} \cdot [H_1H_2A]}{[H^+]} + \frac{K_{a,1,2} \cdot [H_1H_2A]}{[H^+]}\right) \cdot [H^+]}{[H_1H_2A]} = K_{a,1,1} + K_{a,1,2}$	
If $H_1A^- = H_2A^-$ (*i.e.* $K_{a,1,1} = K_{a,1,2}$) then	$K_{a,1} = 2 \cdot K_{a,1,1} \rightarrow \boldsymbol{pK_{a,1} = pK_{a,1,1} - log2}$
Second dissociation	
$(H_2A^- + H_1A^-) \leftrightarrow A^{2-} + H^+$	$K_{a,2} = \frac{[A^{2-}] \cdot [H^+]}{([H_2A^-] + [H_1A^-])}$
$H_2A^- \leftrightarrow A^{2-} + H^+$	$K_{a,2,1} = \frac{[A^{2-}] \cdot [H^+]}{[H_2A^-]}$ $[H_2A^-] = \frac{[A^{2-}] \cdot [H^+]}{K_{a,2,1}}$
$H_1A^- \leftrightarrow A^{2-} + H^+$	$K_{a,2,2} = \frac{[A^{2-}] \cdot [H^+]}{[H_1A^-]}$ $[H_1A^-] = \frac{[A^{2-}] \cdot [H^+]}{K_{a,2,2}}$
$K_{a,2} = \frac{[A^{2-}] \cdot [H^+]}{\left(\frac{[A^{2-}] \cdot [H^+]}{K_{a,2,1}} + \frac{[A^{2-}] \cdot [H^+]}{K_{a,2,2}}\right)} = \frac{K_{a,2,1} \cdot K_{a,2,2}}{K_{a,2,1} + K_{a,2,2}}$	
If $H_1A^- = H_2A^-$ (*i.e.* $K_{a,2,1} = K_{a,2,2}$) then	$K_{a,2} = \frac{K_{a,2,1}}{2} \rightarrow \boldsymbol{pK_{a,2} = pK_{a,2,1} + log2}$
If $H_1A^- \neq H_2A^-$ then	$K_T = \frac{K_{a,1,2}}{K_{a,1,1}} = \frac{K_{a,2,1}}{K_{a,2,2}} = \frac{[H_1A^-]}{[H_2A^-]}$